

PERFLEXMEA: A MULTIELECTRODE ARRAY FOR CELL CULTURE ON A  
THIN PERFORATED FLEXIBLE POLYCARBONATE MEMBRANE

by

Abhijit Mondal

A thesis submitted to the faculty of  
The University of Utah  
in partial fulfillment of the requirements for the degree of

Master of Science

Department of Mechanical Engineering

The University of Utah

August 2011

Copyright © Abhijit Mondal 2011

All Rights Reserved

**The University of Utah Graduate School**

**STATEMENT OF THESIS APPROVAL**

The thesis of Abhijit Mondal

has been approved by the following supervisory committee members:

Alonso P. Moreno, Chair 06/17/2011  
Date Approved

Ian R. Harvey, Member 06/16/2011  
Date Approved

Timothy Ameel, Member 06/17/2011  
Date Approved

and by Timothy Ameel, Chair of  
the Department of Mechanical Engineering

and by Charles A. Wight, Dean of The Graduate School.

## ABSTRACT

Over the past four decades, Multielectrode Array (MEA) devices have played a major role in electrophysiology by providing a simpler solution to simultaneous multi-site chronic extracellular recording: *in vivo* and *in vitro*. While a wide range of devices have been developed, almost all of them are limited to culturing and recording from one cell type, *in vitro*; and tissue surfaces, *in vivo* and *in vitro*. Most tissues are formed by different cell types that interact to maintain tissue function, like the heart which is composed mainly of cardio-myocytes and fibroblasts. Direct recording from such organs usually employs plunge-type electrodes which induce tissue damage and require better handling for sustenance. To better understand the functioning of such tissues, it is imperative to utilize recording systems that allow interactions between two or more cell types and at the same time sustain cultures with controlled cell number and distribution.

In this thesis, the design, fabrication process, and characterization of an MEA device called the PerFlexMEA (Perforated Flexible MEA) is presented. It enables the generation and sustenance of a preparation with two cell types while recording their electrical activity. PerFlexMEA was developed using a thin (9 $\mu\text{m}$ ) perforated Polycarbonate Track Etch (PCTE) membrane (3 $\mu\text{m}$  diam. pores, 200,000 pores/cm<sup>2</sup>) as substrate where cells can be cultured on both sides, allowing gap junction formation across the membrane via the pores. Cell number and distribution can be controlled on either side. The PerFlexMEA comprises a 4  $\times$  5 array of square gold electrodes, each

measuring  $50\ \mu\text{m} \times 50\ \mu\text{m}$  spaced  $500\ \mu\text{m}$  apart. Parylene was patterned to insulate the leads ( $50\ \mu\text{m}$  thick) connecting the recording electrodes to the contact pads. A coin-shaped device was designed to house the PerFlexMEA and to insulate its cell culture zone (wet) from contact pads (dry). Cardiomyocytes, isolated from neonatal mice were plated on the recording side of PerFlexMEA and electrical activity was recorded at a signal to noise ratio of 8.6 and peak to peak voltage of  $200\ \mu\text{V}$ .

This thesis is dedicated to my parents –  
Shri Onkar Nath Mondal and Smt. Priti Kana Mondal.

## TABLE OF CONTENTS

ABSTRACT.....	iii
LIST OF FIGURES.....	ix
LIST OF TABLES.....	xi
ACKNOWLEDGEMENTS.....	xii
Chapter	
1 INTRODUCTION.....	1
1.1 Thesis overview.....	1
1.2 Motivation.....	1
2 RESEARCH BACKGROUND: ELECTROPHYSIOLOGY AND MULTI ELECTRODE ARRAY DEVICES.....	5
2.1 Electrophysiology.....	5
2.1.1 Action potential and conduction velocity.....	6
2.1.2 Excitable cell study.....	11
2.2 Multielectrode Array Devices.....	11
2.2.1 Materials.....	13
2.2.1.1 Substrate.....	13
2.2.1.2 Electrodes.....	14
2.2.1.3 Insulating layer.....	15
2.2.2 Fabrication and Design.....	15
2.2.2.1 Standard MEA devices.....	16
2.2.2.2 High Density MEA.....	17
2.2.2.3 3D MEAs.....	18
2.2.2.4 Flexible MEA devices.....	19
2.2.2.5 Other designs.....	20
2.2.3 Applications.....	24
2.2.4 Summary.....	25
2.3 References.....	26

3	PERFLEXMEA DESIGN.....	30
3.1	Functional requirements.....	30
3.2	Design and materials.....	30
3.2.1	Substrate.....	30
3.2.2	Electrode array, leads and contact pads.....	31
3.2.3	Insulator.....	35
3.2.4	Alignment markers and holes.....	35
3.3	Layer architecture.....	36
3.3.1	Parylene (layer 1).....	36
3.3.2	Gold.....	37
3.3.3	Parylene (layer 2).....	37
3.4	References.....	38
4	FABRICATION.....	39
4.1	Microfabrication process.....	40
4.1.1	Membrane adhesion to rigid substrate.....	40
4.1.2	Parylene deposition – Layer 1.....	42
4.1.3	Pre-etch to promote metal adhesion.....	42
4.1.4	Metal deposition.....	42
4.1.5	Mask generation for lithography.....	44
4.1.6	Gold patterning.....	45
4.1.7	Parylene deposition – Layer 2.....	46
4.1.8	Parylene patterning.....	46
4.1.9	Cutting and reinforcement of alignment holes.....	48
4.1.10	Exfoliation from rigid substrate.....	50
4.2	Characterization.....	52
4.2.1	Layer thickness.....	52
4.2.2	Electrode resistance.....	53
4.3	References.....	55
5	PACKAGING AND INTERFACE.....	56
5.1	The coin setup.....	57
5.2	Amplifier and recording system.....	62
5.2.1	Signal amplification and recording system.....	62
5.2.2	Temperature control system.....	64
5.2.3	Noise reduction set up.....	64



5.2.4 Computer-user interface.....	65
6 PERFORMANCE EXPERIMENTS.....	66
6.1 Biocompatibility.....	66
6.1.1 Cell growth experiment.....	66
6.1.2 Experiment results and discussions.....	67
6.2 Cell coupling across the membrane.....	69
6.2.1 Cell drop experiment.....	69
6.2.2 Experiment results and discussions.....	70
6.3 Electrophysiological recording.....	72
6.3.1 Recording experiment using MEA60 system.....	72
6.3.2 Experiment results and discussions.....	74
6.4 Summary.....	74
6.5 References.....	76
7 SUMMARIZED RESULTS, CONCLUSIONS, FUTURE WORK AND APPLICATIONS.....	77
7.1 Results summary.....	77
7.2 Conclusions.....	78
7.3 Future work.....	78
7.3.1 Design.....	78
7.3.2 Cell specific recipes.....	79
7.4 Future applications.....	79
7.5 Contributions and outcomes.....	81
APPENDICES	
A: MICROFABRICATION PROCESS PARAMETERS.....	82
B: CHARACTERIZATION.....	86
C: CELL GROWTH EXPERIMENT DATA.....	88
D: ISOLATION OF NEONATAL CARDIOMYOCYTES.....	92

## LIST OF FIGURES

Figure	Page
1.1 Thesis structure.....	2
2.1 Giant squid axon action potential.....	7
2.2 Comparison of action potentials using intracellular and extracellular electrodes...	9
2.3 Calculating conduction velocity.....	10
2.4 Standard MEA.....	17
2.5 3D MEAs.....	20
2.6 Flexible multichannel probe array.....	21
2.7 SEM of the cross section of a Neurochip™ well.....	23
2.8 The micro scaffold system.....	23
2.9 Drug effects on ventricular Cardiomyocyte field potentials.....	24
3.1 PCTE membrane.....	32
3.2 PerFlexMEA device design.....	33
3.3 Layer architecture of PerFlexMEA.....	36
4.1 Fabrication steps 1 to 3.....	41
4.2 Membrane adhesion to glass substrate.....	41
4.3 Parylene coating by LPCVD process.....	43
4.4 Reactive ion etching of parylene surface.....	43
4.5 Conductor layer deposition by sputtering.....	43
4.6 Sputtered gold surface.....	44
4.7 Mask patterns.....	45

4.8	Photoresist pattern on metal layer before wet etching .....	46
4.9	Patterning of metal layers.....	47
4.10	Patterned metal layer after wet etching.....	47
4.11	Parylene coating – layer 2.....	48
4.12	Photoresist pattern for parylene patterning.....	49
4.13	Parylene patterning.....	49
4.14	Membrane reinforcement and cutting.....	50
4.15	Soaking of substrate in AZ400K.....	51
4.16	PerFlexMEA after exfoliation.....	51
4.17	SEM images of patterned gold electrodes and parylene on PCTE membrane.....	52
4.18	Measure electrode and stimulator resistances.....	54
5.1	SEI connector aligned to PerFlexMEA contact pads.....	57
5.2	Assembled coin setup housing the PerFlexMEA.....	60
5.3	Exploded view of the coin setup for housing PerFlexMEA.....	61
5.4	SEI one piece interface molded in Sylgard®.....	61
5.5	The amplifier and recording setup.....	63
5.6	The 20 pin convertor for MEA60 system.....	64
6.1	Basic steps of cell growth experiment.....	67
6.2	Cell growth experiment result.....	68
6.3	Cell drop experiment.....	71
6.4	Recorded signals from PerFlexMEA.....	75

## LIST OF TABLES

Table	Page
A.1 PDS 2010 parylene coater process parameters for parylene – layer 1.....	83
A.2 Plasmalab 80 Plus process parameters for parylene (layer 1) surface etch.....	83
A.3 TMV Sputter system process parameters.....	84
A.4 Electromask PG/IR system.....	84
A.5 PDS 2010 parylene coater process parameters for parylene layer – 2.....	85
A.6 Plasmalab 80 Plus process parameters for parylene patterning.....	85
B.1 Thickness of different layer deposition from auxiliary samples.....	87
C.1 Cell count from control Petri dish.....	89
C.2 Cell count from Petri dish with PerFlexMEA.....	90
C.3 Cell count from Petri dish with Sylgard.....	91

## ACKNOWLEDGEMENTS

I would like to begin by thanking the Nora Eccles Harrison Cardiovascular Research and Training Institute and the Treadwell foundation for funding my research. I would like to express my utmost appreciation and gratitude to my advisor, Dr. Alonso P. Moreno for giving me the opportunity of working on this research project with him and for his patience and guidance in this research. My deepest gratitude is extended to my committee members, Dr. Alonso P. Moreno, Dr. Ian R. Harvey and Dr. Timothy Ameel for their valuable input.

Special thanks to Dr. Ian R. Harvey and Brian Baker for their ideas and supervision in the microfabrication of the PerFlexMEA. I am especially grateful to Brian Baker, who has walked me through the fabrication process at the Utah Nanofab facility. I thank the Nanofab staff for their help and support provided in using the sophisticated equipment for the different processes.

I thank Chris Hunter and Rosie Iturralde, Connexin Laboratory for their support and assistance in tissue culture. I also thank Wilson Lobaina, Bruce Steadman and Dennis King, CVRTI, in the design and fabrication of involved electrical circuitry and PerFlexMEA housing apparatus. My regards to Dennis Romney, Machine Shop, Department of Chemistry and Tom Slowik, Machine Shop, Mechanical Engineering for manufacturing the different parts of the PerFlexMEA housing coin.

Finally, I would like to thank the University of Utah for giving me this opportunity to utilize its ample academic and research resources in completing my coursework and research towards a Master of Sciences in Mechanical Engineering. I offer my regards to all those who supported me in any respect during my time at the U.

# CHAPTER 1

## INTRODUCTION

### 1.1 Thesis Overview

In this thesis I present the design, fabrication and characterization of a Multielectrode Array (MEA) device called the Perforated Flexible MEA (PerFlexMEA) that can be used for co-culturing two cell types on either side of a thin perforated polycarbonate flexible membrane and record the electrophysiological activity from the side embedded with a gold MEA. The PerFlexMEA is generated through microfabrication techniques. The design, fabrication and recording properties of electrical activity across murine neonatal myocytes are discussed. Figure 1.1 gives an overview of this thesis.

### 1.2 Motivation

Measurement of extracellular signals from cells and tissues provides vital information in determining cellular excitability and conductive mechanisms. These signals are produced mostly by flow of ions like  $\text{Ca}^+$ ,  $\text{Na}^+$ ,  $\text{K}^+$ ,  $\text{Cl}^-$ , etc. through cell membrane channels. Multi-Electrode Array (MEA) devices have facilitated recordings of such extracellular electrical activity simultaneously from multiple sites, *in vitro* and *in vivo*.

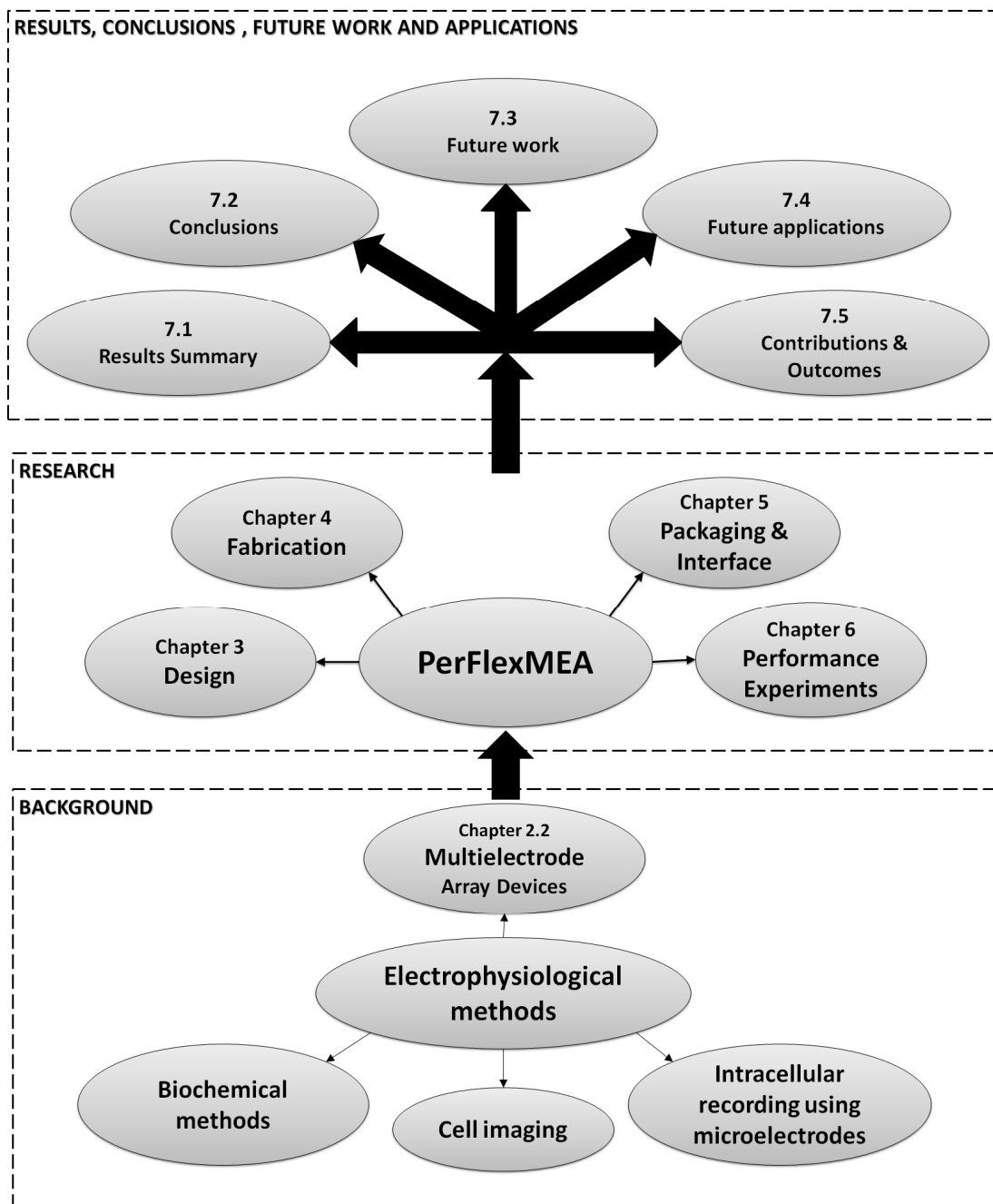


Figure 1.1 Thesis structure. The thesis is divided into three parts – (1) background (2) research and (3) results, conclusions, future work and applications.



MEAs have been extensively used in cardiac and neural research. MEMS (Micro-Electro-Mechanical Systems) technology has played a key role in the development of these devices by offering the ability to create microelectrodes of dimensions  $\sim 10 \mu\text{m}$  and arrays as dense as  $655 \text{ electrodes/mm}^2$  (total of 4096 electrodes).

While photolithography and etching have been the most commonly used techniques for the fabrication of planar electrodes, processes like reactive ion etching (RIE) and deep reactive ion etching (DRIE) have been utilized to craft electrode arrays of 3D-probe-like structures. These electrodes can be plunged into tissues to record at different depths. Biocompatibility and immunogenicity determine the selection of materials for their fabrication. Electrode materials like Pt, Au,  $\text{IrO}_x$ , ITO and TiN have been found to be generally biocompatible when used as electrodes while polymers have been commonly used as insulating layers. Some of these polymers like polyimide, SU-8, parylene and PDMS are flexible and have also been employed to generate flexible electrode arrays. These reduce damage to tissue on implantation and improve recording from convex tissue surfaces.

Current MEA devices are designed for culturing and recording from cells of one type or a mixture of different cell types combined in a two-dimensional scheme. While a major fraction of bodily tissues are composed of two or more cell types (e.g. glia and neurons in the brain, fibroblasts, smooth muscle cells, endothelial cells and myocytes in the heart and endothelial and smooth muscle cells in the arteries), ***there is a need for devices to study preparations where two or more cell types can be co-cultured in a three-dimensional controlled manner.*** Such devices would play a key role in

understanding interaction mechanisms between cells and also for the artificial development of tissues.

## CHAPTER 2

### RESEARCH BACKGROUND: ELECTROPHYSIOLOGY AND MULTIELECTRODE ARRAY DEVICES

#### 2.1 Electrophysiology

Vital organs of the body like the heart, muscles and brain are made of tissues comprising cells capable of producing and responding actively to electrical signals. This type of cells is known as excitable cells. Electrical signals are observed as a result of the flow of ions like those of calcium ( $\text{Ca}^+$ ), potassium ( $\text{K}^+$ ), sodium ( $\text{Na}^+$ ), chloride ( $\text{Cl}^-$ ), etc., controlled by ion channels located on the cell membrane. The various tissues function through the networking of excitable cells and other cell types. Intercellular communication plays a vital role in the physiology of whole organs and systems. Any interference to such communications may lead to organ or system failure. Hence, the study of electrical activity of such tissues at the cellular and tissue level is essential in detecting organ/system malfunctions, and formulating treatments. The branch of physiology that studies the electrical properties and ion movement in biological cells, tissues and organs is known as electrophysiology.

### 2.1.1 Action Potential and Conduction Velocity

An action potential is a short-lasting auto-regenerating event where the membrane potential rapidly decreases and returns to its original potential value. This value is known as the resting membrane potential. The resting membrane potential is the potential difference across the cell membrane in a cell at rest. The resting membrane potential value and action potential characteristics vary from one cell type to another depending on the ionic concentrations across the membrane and the permeability of its active ion channels. The measured action potentials are generated by voltage gated ion channels in the cell membrane. These channels activate or open at the respective threshold voltages, leading to sudden exchange of ions across the membrane. This sudden redistribution of ions leads to changes in potential gradients across the cell membrane observed as action potentials in intracellular or extracellular recordings.

Action potentials play a key role in the functioning of excitable tissues. In the brain, neurons communicate signals from cell to cell using action potentials. In the heart, the action potential results in the release of  $\text{Ca}^+$  ions which cause the heart muscle cells to contract. The generated action potential shape varies from cell type to cell type. It depends on the type of ion channels present and their activation or inactivation voltages. A simple example is the action potential in the giant squid axon, shown in Figure 2.1. The axon being negatively charged inside has a resting potential of -45 mV (shown as dotted line in Figure 2.1). When appropriately stimulated, the sodium channels open up, letting the  $\text{Na}^+$  ions inside the cells, making the cell more positive inside. A sudden rise in membrane potential is recorded (1 to 2 in Figure 2.1). This is known as depolarization. When the membrane potential reaches the respective threshold values, the sodium

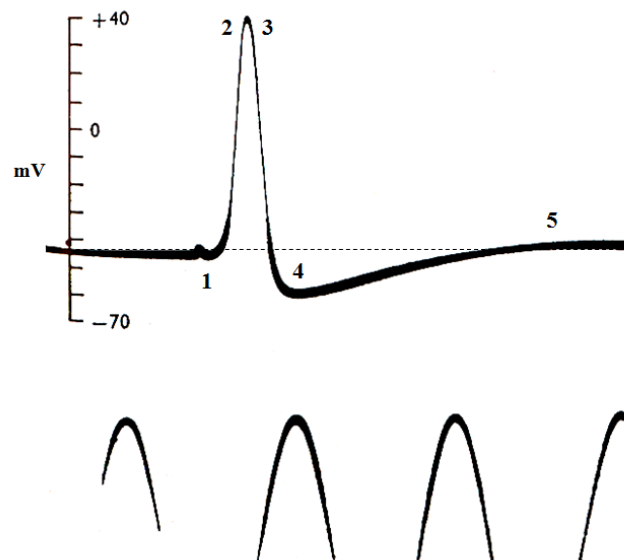


Figure 2.1 Action potential recorded from a giant squid axon using an intracellular electrode. The time scale is represented as a sine wave at 500 Hz. Points 1 to 5 represent the key physiological associated events. (1)  $\text{Na}^+$  channel activation. (2)  $\text{Na}^+$  channel inactivation (3)  $\text{K}^+$  channel activation. (4)  $\text{Na}^+$  and  $\text{K}^+$  pump activation (6) restoration of  $\text{Na}^+/\text{K}^+$  concentration gradients. Reprinted with permission from [1].

channels close and potassium channels opens up (2 to 3 in Figure 2.1). Since the  $\text{K}^+$  channels are slower than the  $\text{Na}^+$  channels, there is a slight delay, seen as a rounded peak. Once the  $\text{K}^+$  channels open, potassium ions are released, causing a drop in the membrane potential (3 to 4 in Figure 2.1). This is known as repolarization. Repolarization generally overshoots the resting potential due to imbalance in concentration gradients of  $\text{Na}^+$  and  $\text{K}^+$  ion across the membrane (4 in Figure 2.1). This is known as hyperpolarization. Next, the sodium and potassium pumps pump sodium out and potassium in, respectively, to maintain the normal ionic concentration gradients and restoring the membrane to the resting potential (4 to 5 in Figure 2.1).

The human ventricular heart cells have a more complicated mechanism involving other ionic channels than sodium, potassium and calcium. Heart cells extracted from

neonatal mice show a simpler action potential curve. Figure 2.2 shows intracellular and extracellular action potentials recorded simultaneously from two different *in vitro* preparations. Since the cell preparation is a mixture of cells from a whole heart, the signal shapes show slight differences.

In the heart, action potentials are transmitted from cell to cell through gap junctions. For proper functioning, the action potentials need to be transmitted to different parts of the heart at a specific rate and speed. The speed at which the action potential (in case of the heart) can be transmitted through the excitable cells (cardiomyocytes) in the tissue is known as the conduction velocity. Conduction velocity is an important parameter in detecting and diagnosing heart diseases like cardiac arrhythmias. The major causes of arrhythmias are conduction abnormalities like partial or complete conduction blockage, re-entry, accessory conduction pathways and fibrillation [3]. These abnormalities can be detected by measuring the conduction velocity at selected regions of the heart. Figure 2.3 shows a simple experiment for calculating conduction velocity along a linearly connected group of cells. Action potentials recorded from each of the connected cells are displaced in time.

Conduction velocity,  $v$  is given by

$$v = \frac{l}{\Delta t}$$

where,  $\Delta t$  is the time delay between action potentials peaks at A and E, and  $l$  is the distance between cell A and E.

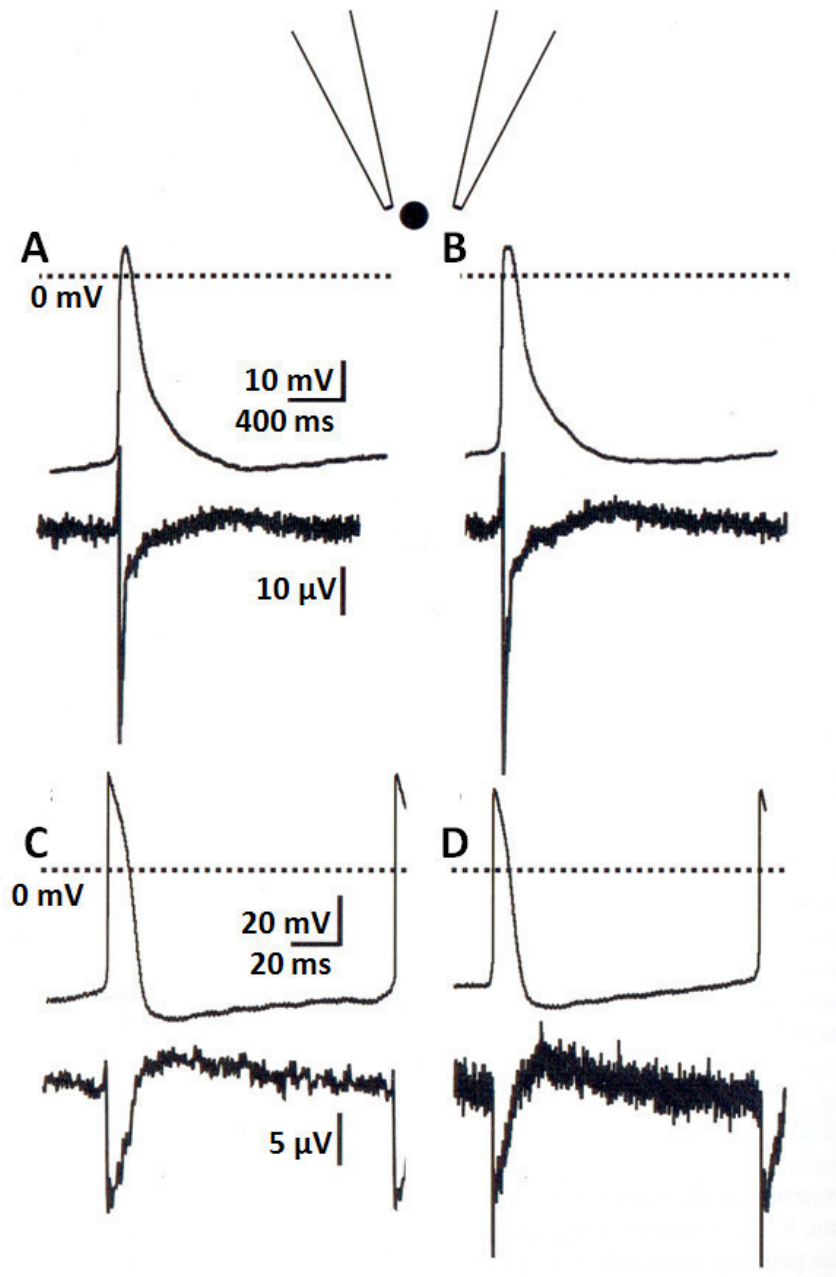


Figure 2.2 Comparison between action potentials recorded using intracellular and extracellular electrodes simultaneously from a heart cell. In each of the paired traces, the upper trace corresponds to the intracellular electrode and lower trace to the extracellular electrode. A, B and C, D are recordings from two different cell preparations. A and B are recording from two different cardiac cells in a preparation. Similarly, C and D are recording from two different cardiac cells from another preparation. Reprinted with permission from [4].

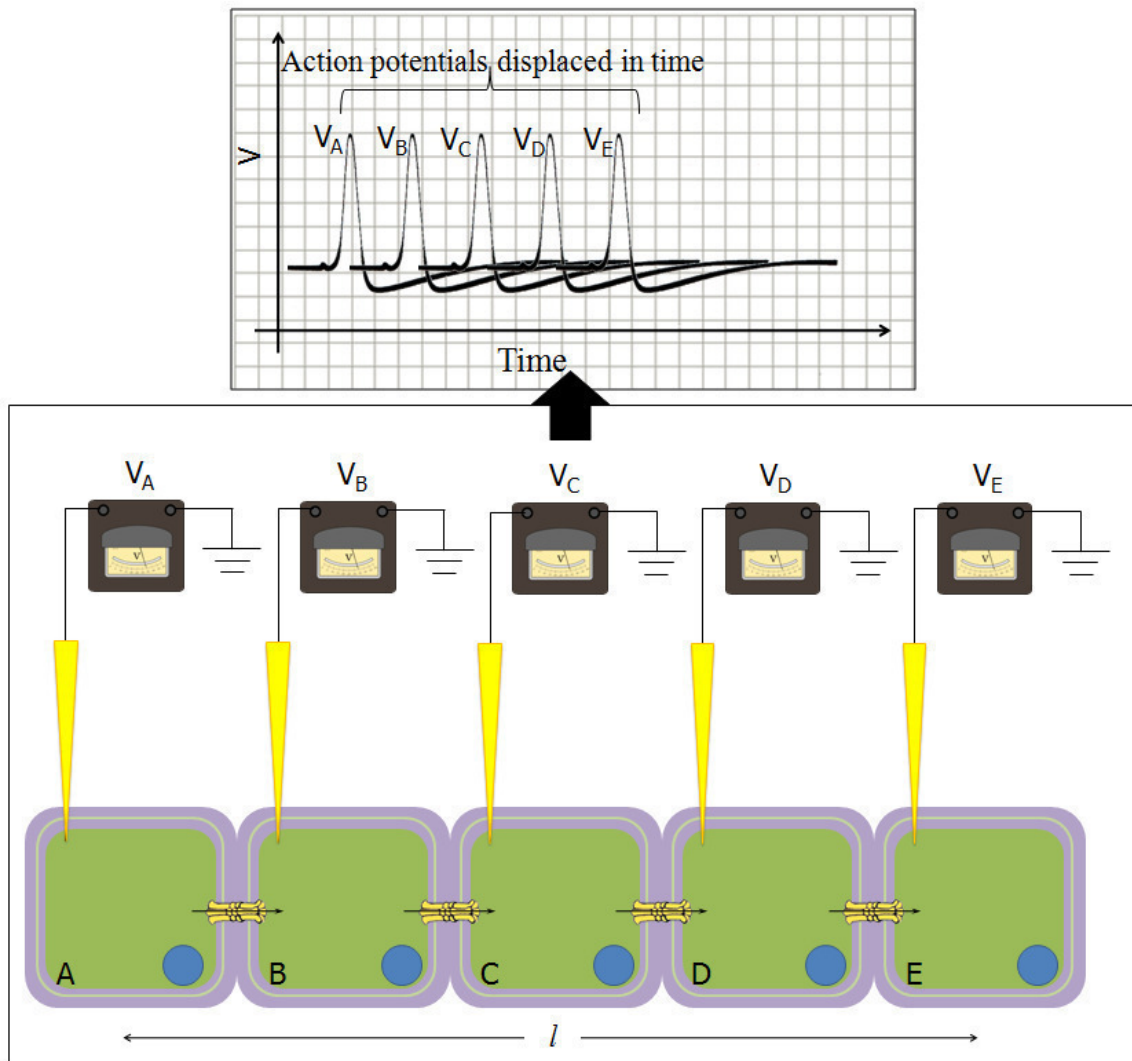


Figure 2.3 Calculating conduction velocity. Cells A to E in the tissue are connected to each other via gap junctions that allow intercellular ion communication. Intracellular measurements using microelectrodes record action potentials at delayed intervals. The time delay between the peaks of the action potentials between cells A and E, and the distance between these cells, are used to calculate the conduction velocity. Modified from [2, 3].



### 2.1.2 Excitable Cell Study

The study of excitable cell needs to be studied using a variety of methods besides electrophysiology, like microscopy, X-ray diffraction methods, radioactive tracing, cell fractional techniques, cell imaging and biochemical methods [2]. Most of these methods are quite complicated and performed using sophisticated equipment. For excitability studies, noninvasive extracellular recording is the simplest way of recording electrophysiological activity from single cells and tissues. Before the invention of Multielectrode Arrays (MEA), probe-like microelectrodes were commonly used for recording electrical signals from cell cultures and tissues. Manipulation of such microelectrodes was cumbersome and required intricate handling by users. Furthermore, cell cultures and tissues under such recording techniques were subjected to harsh environmental conditions such as fluctuating temperature and long exposure to unsterile surroundings, which reduced their survival time, ranging from a few minutes to a few hours. In a tissue, the use of one microelectrode allow limited spatial recording. Recording action potentials from multiple extracellular potentials makes it possible to calculate the conduction velocity and propagation in the heart and this can detect the phenomenology of cardiac diseases.

## 2.2 Multielectrode Array Devices

Multielectrode arrays (also known as microelectrode arrays) are devices with an array or arrays of electrodes employed for recording and stimulating electrical signals from biological tissues and cells. They provide numerous advantages over the conventional methods of electrophysiology. First, they allow the placement of multiple

electrodes concurrently, rather than individually. Second, they enable simultaneous recording from a large number of sites; to date, detection from as many as 4096 sites have been reported [5-7]. Thirdly, the micro-environment for these MEA devices is appropriate to cultured cells and tissues, allowing continuous recordings and in long-term body implants [8-12]. It is also relevant that cell or tissue damage is avoided with a repeated electrode insertion and extraction.

The first MEA device was reported in 1972 and had 30 ( $2 \times 15$ ) platinum black-plated gold microelectrodes, spaced 100  $\mu\text{m}$  apart on glass [13]. A similar device, comprising 36 gold electrodes, spaced 100-200  $\mu\text{m}$  apart, insulated by thermosetting plastic was proposed five years later without the knowledge of previous work [14]. Over the next decade and a half, these devices were successfully used to record from different types of electrogenic cell cultures and tissue and in the last fifteen years, there has been a momentum in the MEA technology development with numerous new MEA devices being reported.

The main source of these developments has been the advancements in microfabrication techniques [15] and materials sciences. Today, many materials can be engineered as per physical, chemical or physiological requirements [16-18]. Lithography and etching are the most common fabrication methods for planar electrode arrays – rigid and flexible. Special processes like Reactive Ion Etching (RIE) and Deep Reactive Ion Etching (DRIE) have enabled fabrication of 3D-probe-like microelectrode arrays. Some of the commercially available MEA systems are manufactured by the Natural and Medical Sciences Institute (NMI, Reutlingen, Germany) [19] , Multi Channel Systems

(MCS, Reutlingen, Germany) [20] and Blackrock Microsystems (Salt Lake City, USA) [21].

In this chapter, some of the different designs, materials used, fabrication methods and applications of MEA devices are discussed.

### 2.2.1 Materials

The two standard criteria for material selection for any biological devices are high biocompatibility and low immunogenicity. “Biocompatibility is defined as the ability of a material to perform with an appropriate response in a specific application, whereas immunogenicity is defined as the ability of the surface to invoke an immune response, such as inflammation” [22]. Properties like high transparency, hydrophilicity, controllable porosity and substrate flexibility are also desirable in many situations.

2.2.1.1 Substrate. Silicon and glass are the most commonly used materials as MEA substrates. Glass is preferred because it is transparent, allowing observation using inverted microscopes. Though it is inexpensive and exhibits excellent chemical and electrical isolation characteristics, not much can be done with glass at the micro-scale. Silicon has emerged as the most popular material for microfabrication with the development of integrated circuits. A study reported silicon to be a biocompatible material that invokes trivial immune response [22]. A variety of fabrication processes can be performed with silicon to obtain diverse structures that can be planar or 3-dimensional [15]. It has been used to fabricate MEA devices with integrated signal amplification and filtering [23]. Polymers such as parylene, polyimide, polyamide, SU-8, etc., are typically used as insulators, but in recent times, their use as substrate in BioMEMS has become

common. They are often inexpensive and offer controllable surface properties such as hydrophobicity, biodegradability and biocompatibility. By varying molecular weight, chemical structures and/or cross-linking densities, properties like biodegradability, drug release kinetics and cell adhesion selectivity can be altered [17, 18]. Thin film flexible polymers like polyimide and polyamide have been used as substrates in a number of flexible MEA devices [11, 18, 24-26]. SU-8 and PDMS have been prominently used in microfluidics and implemented in some special MEA devices [27, 28].

2.2.1.2 Electrodes. Like substrates, electrodes need to be biocompatible and inert to solution contents; at the same time, they should be able to measure small signals with high signal to noise ratio (SNR). Gold, platinum, titanium nitride, iridium oxide and indium-tin oxide (ITO) are commonly used as electrode pads and leads. While the electrode pads do the actual recording from the culture, the leads connect the electrode pads to the amplifying and recording system. Thus, the selected material for the electrode pads has a significant impact on the quality of recorded signal. Electrode material selection is typically application-dependent. Each of the above-mentioned electrode materials possess different material properties (physical and chemical) and electrical characteristics. For example, platinum black and titanium nitride are porous and most suitable for recording very small signal amplitudes [29, 30]. ITO is transparent, hence employed in completely transparent MEAs [31]. Gold exhibits certain cell promoting chemistry [32]. Although platinum black is the most widely used, it shows weak adhesion to base metals and thus wears out with time. Moreover, plating platinum black is a time-consuming process.

2.2.1.3 Insulating layer. Insulation layers are required: (i) to cover the electrode connections and avoid short circuits, (ii) to avoid recording from the leads of the electrode pads and (iii) to isolate any nonbiocompatible material used. Silicon nitride and silicon dioxide were conventionally used by deposition as thin film layers ( $< 1 \mu\text{m}$ ) patterned by photolithography and etching. Such thin layers have been found to be insufficient in eliminating parasitic capacitance. Polymers like polyimide, parylene, SU-8, PDMS, etc., can be deposited with larger thickness and are thus preferred. Polymers too are generally patterned using photolithographic techniques. It has been observed that many of the polymers are biocompatible and invoke low immune responses [22].

### 2.2.2 Fabrication and Design

Since experimental studies utilize devices that record from biological tissue at near cellular resolution, the designed and fabricated electrode features also need to be at similar scales. Thin film deposition and photolithographic patterning are widely used microfabrication techniques utilized for fabrication of planar features [11, 18, 24-26, 29, 33-36]. In photolithography, a pattern is transferred from a mask onto a substrate via localization of UV light, followed by the removal of exposed or unexposed regions using chemicals known as developers. Etching, another widespread technique, is a micromachining process where chemicals like acids and bases (in case of wet etching) or plasmas and gases (in case of dry etching) remove different materials preferentially at different rates. Single crystal silicon expresses directional etch preference. This property of silicon has been tapped where etch techniques, like isotropic and anisotropic etching, have been used to machine specific 3D structures [37-39]. Material deposition is done via

surface micromachining processes – physical vapor deposition (PVD) and chemical deposition (CVD). PVD of metals, alloys or other solid chemical compounds is done by means of thermal energy (evaporation) or ion bombardment (sputtering) in high vacuum. CVD of thin layers of semiconductors or dielectrics ( $< 1 \mu\text{m}$ ) requires a gas phase at low pressures or via high frequency plasma discharges.

Apart from microfabrication, conventional circuit printing (or thick film) technologies have also been employed [13, 29, 40]. These methods generally have limitation of minimum creatable feature size of about 50-100  $\mu\text{m}$  and biocompatibility issues with some of the materials and methods.

Most MEA system designs are application-based and usually governed by the limitations of material fabrication processes.

2.2.2.1 Standard MEA devices. Standard MEA devices are commercially available [19, 20] and generally come in  $8 \times 8$  or  $6 \times 10$  electrode layout grid with 100-500  $\mu\text{m}$  pitch. Titanium nitride electrodes, 10-30  $\mu\text{m}$  in diameter, with titanium or ITO leads are patterned over glass (1 mm thickness). Silicon nitride is used as insulator to cover up the leads. The device is assembled in a standard size of  $49\text{mm} \times 49\text{mm} \times 1 \text{mm}$  with large rectangular contact pads positioned around the edges, connecting the microelectrodes to the amplifier system (Figure 2.4(A)). An MEA system is also available in a hexagonal (Hexa MEA) and denser (High Density MEA) electrode arrangement (Figure 2.4(D)). Though these MEAs are capable of recording from cultures, they are not well suited for use with high powered inverted microscopes. High power objectives with high numerical apertures have a working distance on the order of a few hundreds of micrometers. Hence, the 1 mm thick MEAs become incompatible for use

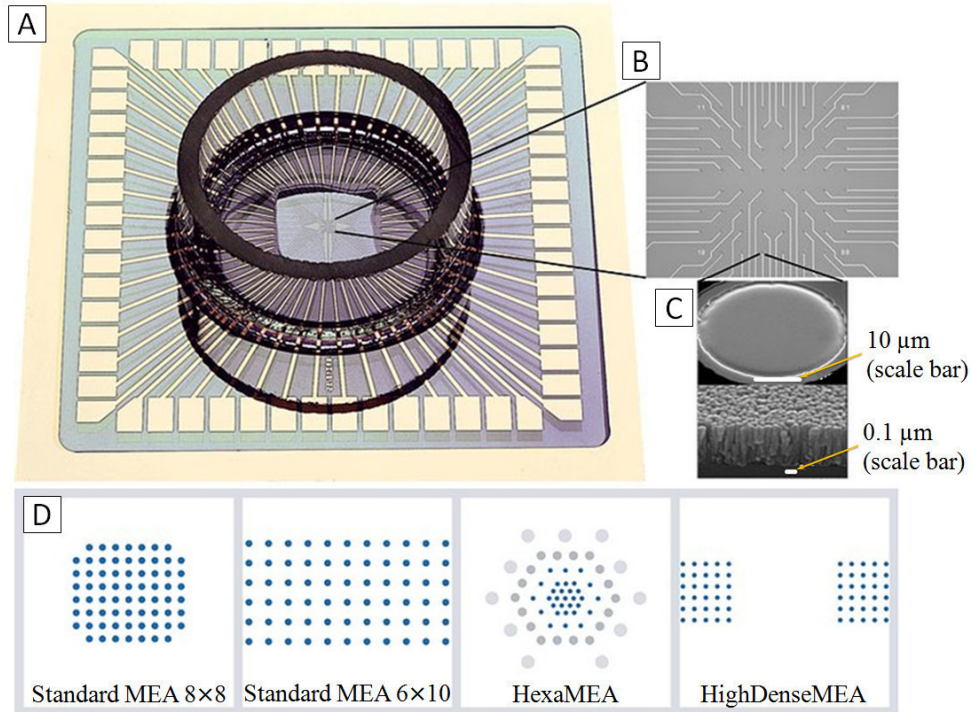


Figure 2.4 Commercially available standard MEA manufactured by Multichannel Systems. (A) The recording electrodes are located at the centre of the glass substrate surrounded by a circular chamber for maintaining culture media. The leads from the recording electrodes extend out of the chamber to the rectangular contact pads designed circumferentially on the glass. (B) Microelectrode array layout with respective leads (C) A single TiN MEA electrode at  $\mu\text{m}$  (top) and  $\text{nm}$  (bottom) resolution. (D) Different available MEA electrode patterns. Electrode patterns (from left to right) for  $8 \times 8$  MEA,  $6 \times 10$  MEA, Hex MEA and High Density MEA. Reprinted with permission from [20].

with these inverted microscopes. To counter this problem, thin MEAs have been developed using  $180 \mu\text{m}$  thick glass substrate mounted on ceramic supports with ITO leads and electrode pads [20, 41]. Electrode arrays with perforated substrates have also been developed. These MEAs allow better circulation of media, nutrients perfusions and gases in cell cultures, improving the environmental conditions, resulting in higher measured amplitudes and longer culture lifespan [23, 42].

2.2.2.2 High density MEA. High density MEAs have been developed using standard complementary-metal-oxide-semiconductor (CMOS) technology with the main

objective of high spatio-temporal resolution imaging of electrophysiological activity in electrogenic cell cultures [7]. A solid-state active pixel sensor (APS) concept was adopted and modified to obtain a high density integrated metallic microelectrode system with on-chip amplification, timing and control circuits and multiplexers. The device contains an array of  $64 \times 64$  gold microelectrodes of  $20\mu\text{m} \times 20\mu\text{m}$ , with underneath pre-amplifiers, over an area of  $2.5\text{ mm} \times 2.5\text{ mm}$  and fabricated using a standard  $0.5\mu\text{m}$  CMOS technology (Alcatel Microelectronics, 5 metal layers technology). The device has reported successful recordings from cardiomyocyte [5, 7] and hippocampal (neurons) cultures [6].

2.2.2.3 3D MEAs. Often when recording from tissue slices, the slice border forms a layer of dead cells. Conventional planar recording systems can only record from outside, making them incapable in such conditions. This problem is overcome using the 3D protruding tip-shaped electrodes [39] as shown in Figure 2.5(A). The electrodes in these arrays generally have probe or needle-like structures which enable them to be immersed into tissues *in vivo* and *in vitro*. The tip shape allows the electrodes to penetrate the dead layer into living cells in the tissue. Therefore, these electrode arrays record larger amplitudes of evoked response when compared to planar ones. The tip-shaped microstructures were fabricated by isotropic etching of glass in HF solution over a mask. The mask protects the glass locally. Initially, the uncovered glass gets etched vertically, followed by under-etching of the mask till it is fully under-etched and detaches. The shape of the mask determines the final shape of the probes. Platinum is deposited on the tips along with the patterned leads, followed by an SU-8 insulation layer. The limitation with the isotropic etching method is that it limits the maximum pitch and aspect ratio



attainable, thus preventing fabrication of tall and dense 3D electrode arrays. BioMEA™ was developed using DRIE on silicon substrate to produce a taller electrode tips array [38]. BioMEA™ has 256 ( $8 \times 32$  matrix) electrodes with a height of 80  $\mu\text{m}$  compared to a 60  $\mu\text{m}$  ( $8 \times 8$  matrix without 4 corner) electrode with height of 60  $\mu\text{m}$  from Heuschkel et al. with same basis of 40  $\mu\text{m}$ . Though BioMEA™ employs the DRIE technique, which is capable of fabricating denser electrode arrays than conventional methods, the fabricated electrode array has the same electrode density as previously reported.

For *in vivo* recordings, longer electrode height is desirable. The Utah Intracortical Electrode Array (Figure 2.5(B)) was one of the first functional electrode arrays that could penetrate  $> 1$  mm [43]. Other devices have also been reported by microassembly of multishank planar silicon probes [8] and using silicon-on-insulator (SOI) [44]. Most of these electrode arrays, though 3D structured, record electrical signals mostly from planar profiles.

2.2.2.4 Flexible MEA devices. Flexible MEA devices are increasingly becoming common for recording *in vivo* [11], and from tissue slices *in vitro* [24]. These devices enable electrical measurements with reduced trauma to the tissue, are easier to locate and eliminate the limitations of flat surface recording. The electrode array can be wrapped around or cast into the basic shape of the tissue. Perforations near recording sites are a supplementary gain and increases lifespan of the cultures [24]. While conventional MEA systems enable only two-dimensional recording, flexible electrode array devices enable recording in a three-dimensional surface level. Flexible materials have also been utilized to fabricate implantable electrodes capable of recording in 3D [18, 26]. These electrode arrays combine the benefits of 3D-probe-like and flexible MEAs. In addition to reducing

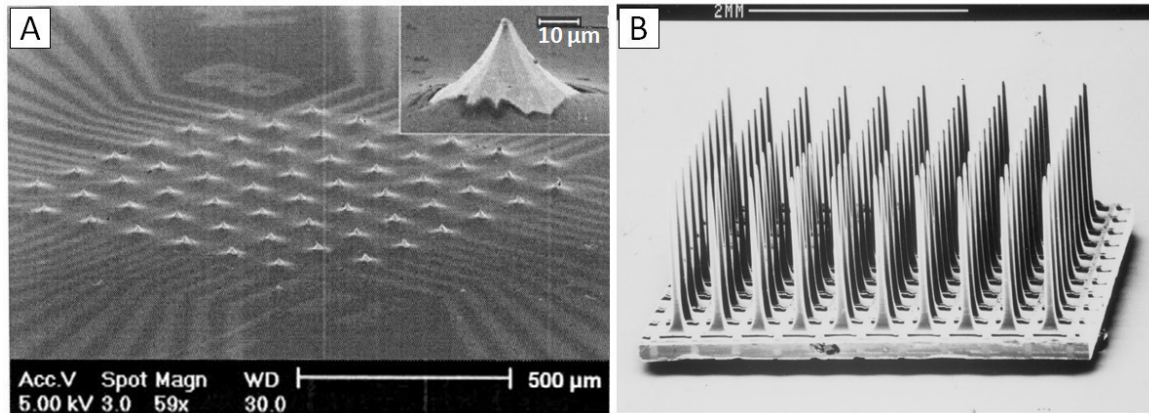


Figure 2.5 3D MEAs. (A) SEM image of a 3D MEA recording area composed of 60 tip-shaped platinum electrodes and thin epoxy layer as insulator. The 3D pointed structures were formed by reactive ion etching of glass. The pointed electrodes are 60  $\mu\text{m}$  in height with 40  $\mu\text{m}$  diameter base. Reprinted with permission from [39]. (B) SEM image of the Utah Intracortical Electrode Array. The microelectrodes are longer than 1mm. Their height enables them to be plunged into tissues for recording at different depths. Reprinted with permission from [9].

trauma to tissue, they have the ability to record at different depths. Being flexible, maintaining these probes in a straight line would be problematic as they might have a tendency to fold or curl. Furthermore, flexible MEAs are fabricated on thin films (10-100  $\mu\text{m}$ ) that are delicate. They wear off easily and are unsuitable for multiple uses. Takeuchi et al. [26] have used magnetic thin plates on the backside of the probes (Figure 2.6). This improves their stiffness and enables them to be easily folded by application of magnetic field, which can be utilized for batch assembly.

2.2.2.5 Other designs. Apart from the above-discussed devices, there are quite a few other MEA devices which have demonstrated unique capabilities. For example, the Neurochip [37] was developed, with a  $4 \times 4$  electrode array where each electrode had caged well-like structures (Figure 2.7) to locate single neurons while also permitting normal growth and functionality. Platinum black plated gold electrodes were used as

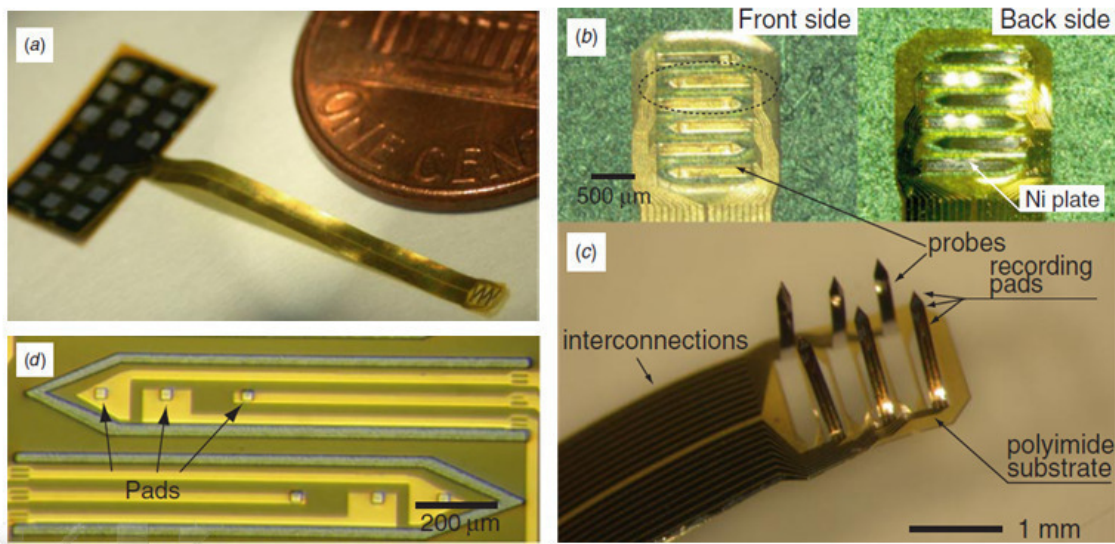


Figure 2.6 Flexible multichannel probe array. (a) The entire probe array is about 2 cm in length. (b) Front and back side of the probe array before folding. (c) 3D flexible probe array after folding. (d) Recording pads of each probes. Each probe has 3 recording pads arranged height-wise enabling it to record from different depths. Reprinted with permission from [26].

electrode pads which enhanced recording quality, enabling electrical signal measurements with high SNR values of 35-70. Cell localization into these well-like structures had to be physically or mechanically done using glass micro-pipettes with sealed tips. This would be a laborious process, comparable to those of manipulating and recording using traditional single electrode needles. Furthermore, washing the caged structures after recording experiments would be tricky, increasing the likelihood of postexperimental residues, resulting in contamination of preparation on multiple uses.

A Microfabricated Compartmented Culture System ( $\mu$ -CCS) [33, 34] was developed where neurons could be grown with extensions spread into adjacent compartments, while sustaining fluid isolation amongst compartments. The substrate had thin film collagen coated lines that direct neuron growth and movement along adjoining electrode paths.

An MEA device with integrated heater and temperature sensor has been developed [40]. Conventional external culture temperature control systems are quite bulky compared to this device. Commercial flexible printed circuit board (flex-PCB) technology was used over microfabrication, reducing the cost of production. The device was aimed for single-use: flex-PCB methods being more rugged and unclean compared to microfabrication methods. Throwing away such integrated systems after a single use is not resourceful.

Rowe et al. have developed an electrical recording system in an active 3D scaffold system with fluid perfusion for culturing of neurons in 3D [27]. The device (Figure 2.8) is assembled by attaching  $8 \times 8$  arrays of hollow SU-8 towers to horizontal SU-8 cross-members connecting the neighboring towers. This enhances the growth and branching of hippocampal neurons in all direction in the 3D grid. Hollow channels in the scaffolds are used to deliver media and nutrient perfusions to the cell culture. Electrical signals are recorded using the two exposed gold electrodes (with insulated leads) located at the outer wall of each tower at different heights.

While most *in vitro* devices reported to date record in 2D, some *in vivo* application devices are able to record in sparser 3D arrays. The microscaffold system has the potential of culturing and recording in 3D. The number of simultaneous recordable electrodes in such designs would be a limiting factor and could require more sophisticated systems. This system also lacks the control of cell patterning in all three directions. However, technology for cell patterning in 2D is already available.

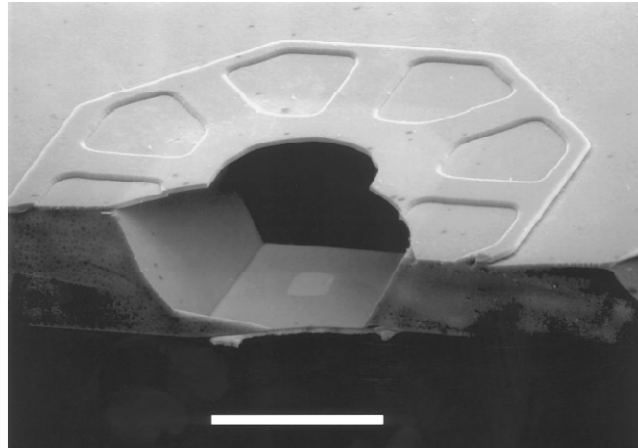


Figure 2.7 SEM of the cross-section of a Neurochip™ well. The scale bar is 20  $\mu\text{m}$  long. The recording electrode is located at the floor of the well where the neuron is located. The caged well-structure provides better shielding against external noise enabling recording at high SNR (35-70). Reprinted with permission from [37].

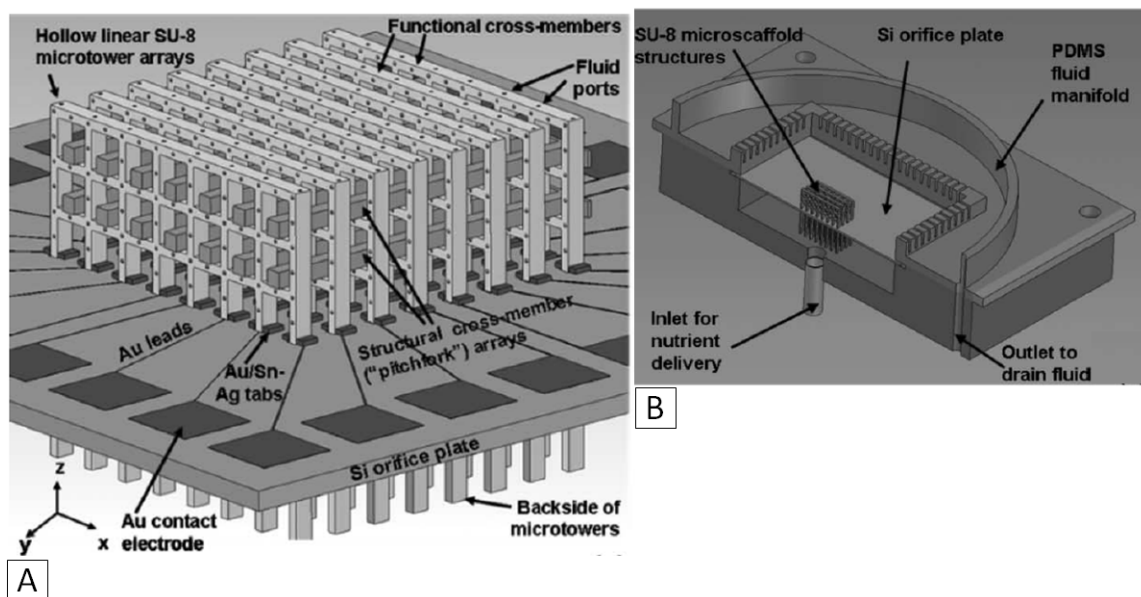


Figure 2.8 A 3D microcylinder array with recording system. (a) An  $8 \times 8$  array of hollow microcylinders with cross-connects along x-direction and y-direction projecting out the topside and backside of the Si orifice plate. (b) 3-D cross-sectional view of the microcylinder array installed in the PDMS manifold. Reprinted with permission from [27].

### 2.2.3 Applications

Apart from recording/stimulation from/of electrogenic cells, in the last decade, MEA technology has also shown applications in biosensor development. Stett et al. have reviewed some of the biological applications of MEA in drug discovery using cardiomyocyte cultures, explanted retinas and neurons (brain slices) [10]. Figure 2.9 shows the effects of few drugs at various concentrations to the measured action potential from ventricular cardiomyocyte cultures. Neurons in particular possess a great potential in cell-based biosensors as they express sensitivity towards odors, drugs and toxins by changes in recordable cellular electrical activity [17]. They tend to bind to these

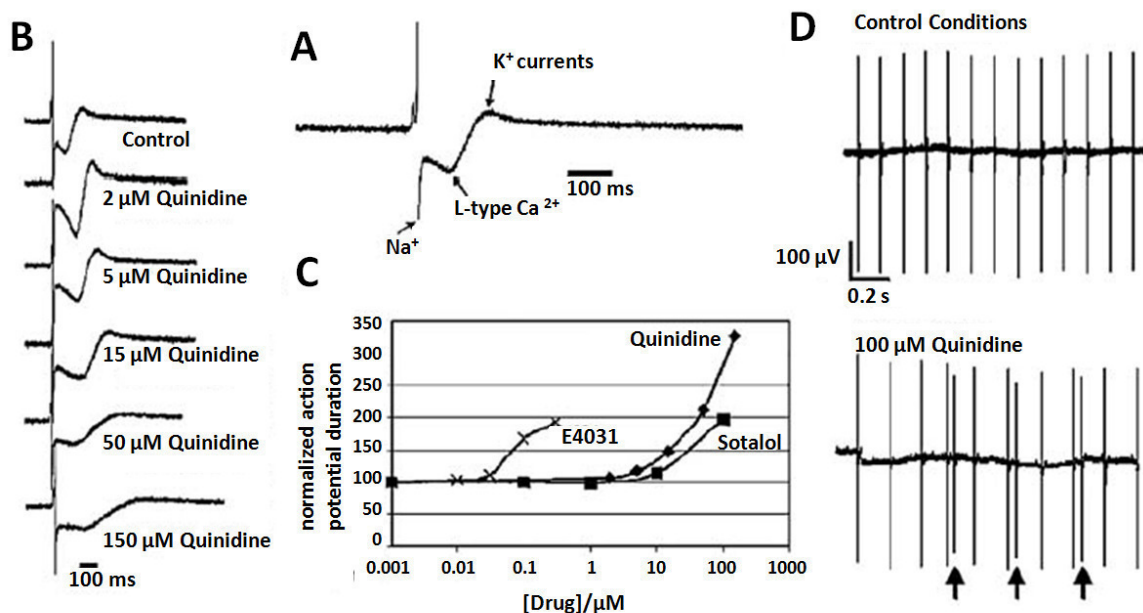


Figure 2.9 Drug effects on ventricular cardiomyocyte action potential duration. (A) Extracellular field potential under controlled conditions. (B) Potentials recorded at different concentrations of quinidine. (C) Effect of different drugs at different concentration on the extracellular field potential duration. (D) Distortion in rhythm due to quinidine. The arrows point to early after potentials (EAD). Reprinted with permission from [10].

substances to generate substance-specific and concentration-dependent responses. Appropriate data analysis of these responses can be used to trigger sensor output.

#### 2.2.4 Summary

Review of literature has shown that MEA technology has been a reliable tool for electrophysiological recordings with high information content with respect to electrogenic cell mechanisms and drug action in controlled cellular environments. Microfabrication technology enables us to create high density, biocompatible and application-specific electrode systems. Development of new materials and fabrication methods has increased the range of options for scientists. While a variety of devices have been developed, most *in vitro* MEA devices have been designed for culturing and recording from only one cell type, some devices can culture two or more cell types in two-dimensional schemes which involve advanced cell patterning techniques to control cell distribution. Since most bodily tissues are made of two or more cell types, there is a need for MEA devices that are capable of co-culturing two cell types with simpler ways to control cell distribution and patterning. Such devices would simplify studying the effects of varying cell distribution in excitable tissues.

### 2.3 References

- [1] A. L. Hodgkin and A. F. Huxley, "Resting and action potentials in single nerve fibres.," *J Physiol*, vol. 104, pp. 176-95, Oct 1945.
- [2] D. J. Aidley, *The physiology of excitable cells*, 4th ed. Cambridge, UK ; New York, NY, USA: Cambridge University Press, 1998.
- [3] W. F. Boron and E. L. Boulpaep, *Medical Electrophysiology*, Updated edition ed. Philadelphia, PA: Elsevier Saunders, 2005.
- [4] M. Halbach, U. Egert, J. Hescheler, and K. Banach, "Estimation of action potential changes from field potential recordings in multicellular mouse cardiac myocyte cultures.," *Cell Physiol Biochem*, vol. 13, pp. 271-84, 2003.
- [5] K. Imfeld, S. Neukom, A. Maccione, Y. Bornat, S. Martinoia, P. A. Farine, M. Koudelka-Hep, and L. Berdondini, "Large-scale, high-resolution data acquisition system for extracellular recording of electrophysiological activity," *IEEE Trans Biomed Eng*, vol. 55, pp. 2064-73, Aug 2008.
- [6] L. Berdondini, K. Imfeld, A. Maccione, M. Tedesco, S. Neukom, M. Koudelka-Hep, and S. Martinoia, "Active pixel sensor array for high spatio-temporal resolution electrophysiological recordings from single cell to large scale neuronal networks," *Lab Chip*, vol. 9, pp. 2644-51, Sep 21 2009.
- [7] L. Berdondini, P. D. van der Wal, O. Guenat, N. F. de Rooij, M. Koudelka-Hep, P. Seitz, R. Kaufmann, P. Metzler, N. Blanc, and S. Rohr, "High-density electrode array for imaging in vitro electrophysiological activity," *Biosens Bioelectron*, vol. 21, pp. 167-74, Jul 15 2005.
- [8] A. C. Hoogerwerf and K. D. Wise, "A three-dimensional microelectrode array for chronic neural recording," *IEEE Trans Biomed Eng*, vol. 41, pp. 1136-46, Dec 1994.
- [9] P. J. Rousche and R. A. Normann, "Chronic recording capability of the Utah Intracortical Electrode Array in cat sensory cortex," *J Neurosci Methods*, vol. 82, pp. 1-15, Jul 1 1998.
- [10] A. Stett, U. Egert, E. Guenther, F. Hofmann, T. Meyer, W. Nisch, and H. Haemmerle, "Biological application of microelectrode arrays in drug discovery and basic research," *Analytical and Bioanalytical Chemistry*, vol. 377, pp. 486-495, Oct 2003.
- [11] B. A. Hollenberg, C. D. Richards, R. Richards, D. F. Bahr, and D. M. Rector, "A MEMS fabricated flexible electrode array for recording surface field potentials," *J Neurosci Methods*, vol. 153, pp. 147-53, May 15 2006.
- [12] K. Molina-Luna, M. M. Buitrago, B. Hertler, M. Schubring, F. Haiss, W. Nisch, J. B. Schulzad, and A. R. Luft, "Cortical stimulation mapping using epidurally



- implanted thin-film microelectrode arrays," *Journal of Neuroscience Methods*, vol. 161, pp. 118-125, Mar 30 2007.
- [13] C. A. Thomas, Jr., P. A. Springer, G. E. Loeb, Y. Berwald-Netter, and L. M. Okun, "A miniature microelectrode array to monitor the bioelectric activity of cultured cells," *Exp Cell Res*, vol. 74, pp. 61-6, Sep 1972.
- [14] G. W. Gross, E. Rieske, G. W. Kreutzberg, and A. Meyer, "A new fixed-array multi-microelectrode system designed for long-term monitoring of extracellular single unit neuronal activity in vitro," *Neurosci Lett*, vol. 6, pp. 101-5, Nov 1977.
- [15] M. J. Madou, *Fundamentals of microfabrication*. Boca Raton, Fla.: CRC Press, 1997.
- [16] G. C. Engelmayr, M. Y. Cheng, C. J. Bettinger, J. T. Borenstein, R. Langer, and L. E. Freed, "Accordion-like honeycombs for tissue engineering of cardiac anisotropy," *Nature Materials*, vol. 7, pp. 1003-1010, Dec 2008.
- [17] T. H. Park and M. L. Shuler, "Integration of cell culture and microfabrication technology," *Biotechnology Progress*, vol. 19, pp. 243-253, Mar-Apr 2003.
- [18] P. J. Rousche, D. S. Pellinen, D. P. Pivin, Jr., J. C. Williams, R. J. Vetter, and D. R. Kipke, "Flexible polyimide-based intracortical electrode arrays with bioactive capability," *IEEE Trans Biomed Eng*, vol. 48, pp. 361-71, Mar 2001.
- [19] *Natural and Medical Sciences Institute* [website]. Available: [www.nmi1.de](http://www.nmi1.de)
- [20] *Multi Channel Systems*. Available: [www.multichannelsystems.com](http://www.multichannelsystems.com)
- [21] *Blackrock Microsystems*. Available: <http://www.blackrockmicro.com/>
- [22] K. M. Ainslie and T. A. Desai, "Microfabricated implants for applications in therapeutic delivery, tissue engineering, and biosensing," *Lab on a Chip*, vol. 8, pp. 1864-1878, 2008.
- [23] P. Thiebaud, N. F. de Rooij, M. Koudelka-Hep, and L. Stoppini, "Microelectrode arrays for electrophysiological monitoring of hippocampal organotypic slice cultures," *IEEE Trans Biomed Eng*, vol. 44, pp. 1159-63, Nov 1997.
- [24] S. A. Boppart, B. C. Wheeler, and C. S. Wallace, "A flexible perforated microelectrode array for extended neural recordings," *IEEE Trans Biomed Eng*, vol. 39, pp. 37-42, Jan 1992.
- [25] C. Gonzalez and M. Rodriguez, "A flexible perforated microelectrode array probe for action potential recording in nerve and muscle tissues," *J Neurosci Methods*, vol. 72, pp. 189-95, Apr 4 1997.
- [26] S. Takeuchi, T. Suzuki, K. Mabuchi, and H. Fujita, "3D flexible multichannel neural probe array," *Journal of Micromechanics and Microengineering*, vol. 14, pp. 104-107, Jan 2004.

- [27] L. Rowe, M. Almasri, K. Lee, N. Fogleman, G. J. Brewer, Y. Nam, B. C. Wheeler, J. Vukasinovic, A. Glezer, and A. B. Frazier, "Active 3-D micro scaffold system with fluid perfusion for culturing in vitro neuronal networks," *Lab Chip*, vol. 7, pp. 475-82, Apr 2007.
- [28] B. J. Dworak and B. C. Wheeler, "Novel MEA platform with PDMS microtunnels enables the detection of action potential propagation from isolated axons in culture," *Lab Chip*, vol. 9, pp. 404-10, Feb 7 2009.
- [29] H. Oka, K. Shimono, R. Ogawa, H. Sugihara, and M. Taketani, "A new planar multielectrode array for extracellular recording: application to hippocampal acute slice," *Journal of Neuroscience Methods*, vol. 93, pp. 61-67, Oct 30 1999.
- [30] U. Egert, B. Schlosshauer, S. Fennrich, W. Nisch, M. Fejtl, T. Knott, T. Muller, and H. Hammerle, "A novel organotypic long-term culture of the rat hippocampus on substrate-integrated multielectrode arrays," *Brain Res Brain Res Protoc*, vol. 2, pp. 229-42, Jun 1998.
- [31] J. P. Kucera, M. O. Heuschkel, P. Renaud, and S. Rohr, "Power-law behavior of beat-rate variability in monolayer cultures of neonatal rat ventricular myocytes," *Circ Res*, vol. 86, pp. 1140-5, Jun 9 2000.
- [32] Y. Nam, J. C. Chang, B. C. Wheeler, and G. J. Brewer, "Gold-coated microelectrode array with thiol linked self-assembled monolayers for engineering neuronal cultures," *IEEE Trans Biomed Eng*, vol. 51, pp. 158-65, Jan 2004.
- [33] S. K. Ravula, M. A. McClain, M. S. Wang, J. D. Glass, and A. B. Frazier, "A multielectrode microcompartment culture platform for studying signal transduction in the nervous system," *Lab on a Chip*, vol. 6, pp. 1530-1536, Dec 2006.
- [34] S. K. Ravula, M. S. Wang, S. A. Asress, J. D. Glass, and A. B. Frazier, "A compartmented neuronal culture system in microdevice format," *Journal of Neuroscience Methods*, vol. 159, pp. 78-85, Jan 15 2007.
- [35] A. Mohr, W. Finger, K. J. Fohr, W. Gopel, H. Hammerle, and W. Nisch, "Performance of a thin film microelectrode array for monitoring electrogenic cells in vitro," *Sensors and Actuators B-Chemical*, vol. 34, pp. 265-269, Aug 1996.
- [36] A. E. Grumet, J. L. Wyatt, Jr., and J. F. Rizzo, 3rd, "Multi-electrode stimulation and recording in the isolated retina," *J Neurosci Methods*, vol. 101, pp. 31-42, Aug 15 2000.
- [37] M. P. Maher, J. Pine, J. Wright, and Y. C. Tai, "The neurochip: a new multielectrode device for stimulating and recording from cultured neurons," *J Neurosci Methods*, vol. 87, pp. 45-56, Feb 1 1999.

- [38] G. Charvet, O. Billoint, L. Rousseau, and B. Yvert, "BioMEA: a 256-channel MEA system with integrated electronics," *Conf Proc IEEE Eng Med Biol Soc*, vol. 2007, pp. 171-4, 2007.
- [39] M. O. Heuschkel, M. Fejtl, M. Raggenbass, D. Bertrand, and P. Renaud, "A three-dimensional multi-electrode array for multi-site stimulation and recording in acute brain slices," *J Neurosci Methods*, vol. 114, pp. 135-48, Mar 15 2002.
- [40] L. Giovangrandi, K. H. Gilchrist, R. H. Whittington, and G. T. A. Kovacs, "Low-cost microelectrode array with integrated heater for extracellular recording of cardiomyocyte cultures using commercial flexible printed circuit technology," *Sensors and Actuators B-Chemical*, vol. 113, pp. 545-554, Jan 17 2006.
- [41] D. Eytan, A. Minerbi, N. Ziv, and S. Marom, "Dopamine-induced dispersion of correlations between action potentials in networks of cortical neurons," *J Neurophysiol*, vol. 92, pp. 1817-24, Sep 2004.
- [42] U. Egert, S. Okujeni, W. Nisch, B. K-H, R. R, G. N, and A. Stett, "Perforated Microelectrode Arrays Optimize Oxygen Availability and Signal-to-Noise Ratio in Brain Slice Recordings," presented at the Mikrosystemtechnologie Kongress Freiburg, 2005.
- [43] K. E. Jones, P. K. Campbell, and R. A. Normann, "A glass/silicon composite intracortical electrode array," *Ann Biomed Eng*, vol. 20, pp. 423-37, 1992.
- [44] C. H. Chen, D. J. Yao, S. H. Tseng, S. W. Lu, C. C. Chiao, and S. R. Yeh, "Micro-multi-probe electrode array to measure neural signals," *Biosens Bioelectron*, vol. 24, pp. 1911-7, Mar 15 2009.

## CHAPTER 3

### PERFLEXMEA DESIGN

#### 3.1 Functional Requirements and Objectives

The PerFlexMEA has three core functional objectives.

1. *Co-culture of two cell types*: The device should be able to co-culture two cell types independently in a controlled manner in terms of cell number and distribution.
2. *Gap junction formation*: It should permit the formation of gap junctions between the two cell types across the membrane to enable direct communication.
3. *Recording electrical activity*: It should be capable of recording electrical activity from the selected cell type from the preparation.

#### 3.2 Design and Materials

The MEA device was designed to fulfill the functional objectives taking into consideration the constraints in dimensions, accessible materials and fabrication methods. The device design and constraints are discussed in the following sections.

##### 3.2.1 Substrate

The PCTE membrane was the primary candidate as a substrate as it fulfilled the first two functional objectives – capability of growing two distinct cell types

simultaneously at each side and permitting communication across the membrane. Another important constraint was cell migration across the membrane. Selecting a thin membrane with 3  $\mu\text{m}$  diameter holes prevented cellular migration [3]. The Polycarbonate Track Etch (PCTE) membrane<sup>1</sup> (shown in Figure 3.1) was selected as substrate. The PCTE membrane was 9  $\mu\text{m}$  thick with 3  $\mu\text{m}$  diameter pores and 200,000 pores/cm<sup>2</sup> pore density. These membranes have been reported to be biocompatible with different cell cultures and used for a wide range of experiments. These and other types of membrane products are available commercially [1]. The selected PCTE membranes from Sterlitech Corp. were inexpensive when compared to the other commercially available products. Being extremely thin and porous enables cells plated at both sides of the membrane to form gap junctions and communicate across the membrane [2]. Thus, PCTE membrane became the primary source of design constraints in the recording device dimensions, fabrication method (discussed in Section 4.1), packaging and interfacing (discussed in Section 5.1).

### 3.2.2 Electrode Array, Leads and Contact Pads

Gold was selected as the conductor layer for patterning the electrode array, leads and contact pads due to its favorable physical and chemical properties. Gold has high conductivity and chemical inertness, making it an excellent choice of material for recording electrodes and leads. Furthermore, gold is highly malleable, ductile and can be easily deposited and patterned. These positive characteristics of gold have made it widely used as electrode material for flexible MEA devices [6-10]. Titanium and titanium dioxide layers were also deposited below gold to promote gold adhesion.

---

<sup>1</sup> Sterlitech Corp., Kent, USA

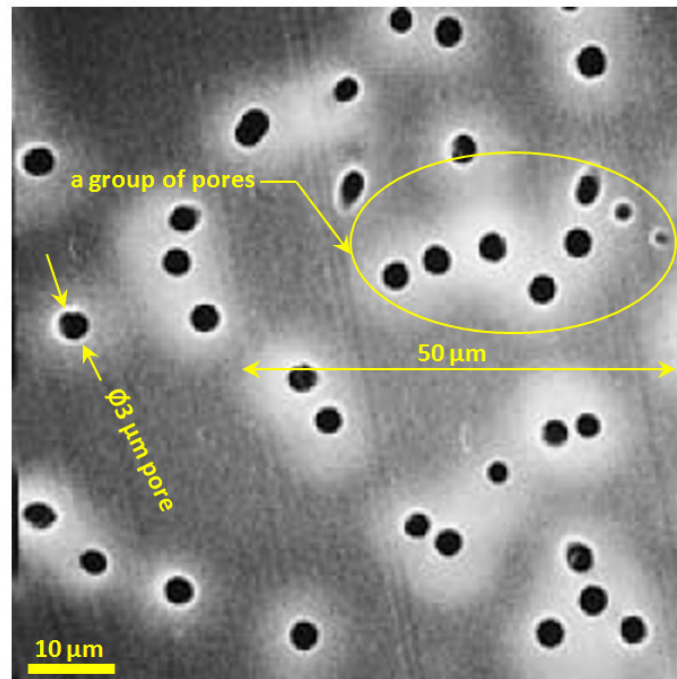


Figure 3.1 Polycarbonate track etch or PCTE membrane manufactured by Sterlitech Corp. The membrane has 3  $\mu\text{m}$  diameter pores randomly distributed with 20,000 pores/ $\text{cm}^2$  pore density. Some sections of the membrane have groups of pores (marked in circular region) which was an important factor in determining the electrode and lead dimensions. Taken with permission from ref. [4].

To meet functional objectives 1 and 2, a porous substrate was imperative. This restricted the minimum selectable recording electrode size and lead thickness. The PCTE membrane was observed to have regions where pores were closely located. Leads or electrodes in such sections would have high resistance, resulting in deterioration of signal quality. Figure 3.1 shows one such case (circled). To avoid such high resistance sections, the electrode and lead widths were set to 50  $\mu\text{m}$ . This offered sufficient conduction width and reduced the section's resistance.

Based on the selected 50  $\mu\text{m}$  width, a  $4 \times 5$  array of square electrodes of side 50  $\mu\text{m}$  spaced 500  $\mu\text{m}$  apart (Figure 3.2(E)) was designed (Figure 3.2(D)) to create a

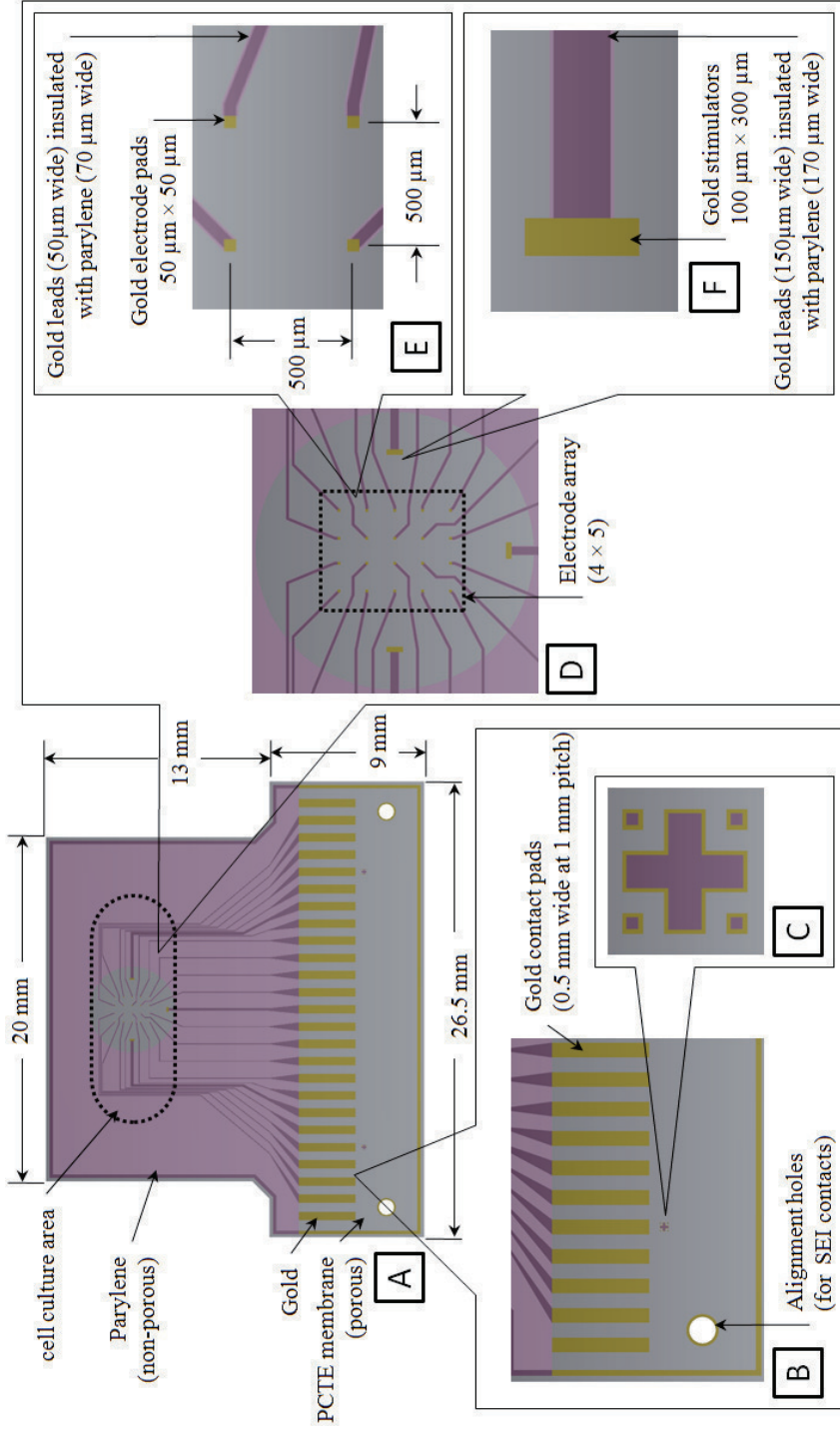


Figure 3.2 PerFlexMEA device design. (A) The structural layout of the device on the PCTE membrane. The regions in pink represent parylene coating on top. (B) A close up view of the contact pads and alignment holes. The SEI connectors align to the contact pads with its pins located in the alignment holes. (C) Alignment marks used for patterning the parylene layer over gold. (D) The porous (grey colored region) cell culture zone with the  $4 \times 5$  recording electrode array and the 3 stimulating electrodes. (E) Square recording electrode size and pitch. (F) Rectangular stimulating electrode size.

recording area of  $2 \text{ mm} \times 2.5 \text{ mm}$ . A pitch of  $500 \text{ }\mu\text{m}$  reserved approximately 10000 pores in the electrode array region. The actual number might be less than 10000 as the area covered by the electrodes and leads was nonporous. Since electrode shape does not have much functional affect, the electrodes were patterned as squares to facilitate its design. Selecting square over circular electrodes reduces the cost and time in mask generation for fabrication. The electrode array was positioned at the centre of the cell culture zone. The centre of the cell culture zone had a circular region of  $5 \text{ mm}$  diameter where the membrane was porous. Three stimulation gold electrodes (Figure 3.2(F)) of size  $100 \text{ }\mu\text{m} \times 300 \text{ }\mu\text{m}$  were located at the centers of three sides of the array. The electrode array had 20 recording electrodes and 3 stimulating electrodes. The number of electrodes and stimulators were selected based on the available size and number of pins of commercially available SEI coiled connector [5] used for interfacing. A 25-pin SEI connector was selected as it could be packaged into the coin setup (discussed in Section 5.1) to fit in a  $60 \text{ mm}$  Petri dish. The recording and stimulating electrodes were connected to the amplification and data acquisition system via larger contact pads, as shown in Figure 3.2(B). Each electrode was connected to its respective contact pad by  $50 \text{ }\mu\text{m}$  thin leads. The contact pads were arranged in a linear array of  $0.5 \text{ mm} \times 3.3 \text{ mm}$  rectangular pads and  $1 \text{ mm}$  pitch. The main constraint in the design of the contact pads was the use of commercially available coiled connectors (SAMTEC SEI one piece interface [5]) that were required to sit on each of the contact pads which were in turn connected to the amplification and data acquisition system. The coiled connectors from the SEI one piece interface sat on their respective contact pads.



### 3.2.3 Insulator

Parylene was selected to be used as insulator. It can be suitably deposited to form a thin flexible layer ( $< 1\mu\text{m}$ ) and had been reported to be biocompatible [11-13]. To insulate the leads, parylene was patterned on the gold surfaces – top and bottom. The pink colored pattern in Figure 3.2 represents parylene. While the leads were insulated on both sides – top and bottom, the recording electrode pads were insulated only at the bottom (as shown in Figure 3.3). This prevented any recording from the leads and restricts the electrode pads to recording only from the top surface. The parylene blocks the pores throughout the patterned conductor region. In the cell culture zone (Figure 3.2(D)-(E)) the parylene over the leads was patterned to cover them and extend  $10\mu\text{m}$  wider on each side (insulator over lead width =  $70\mu\text{m}$ ). The extra width ensures total lead insulation.

### 3.2.4 Alignment Markers and Holes

Figure 3.2(C) shows the cross-shaped alignment marks. These marks are used as reference to align the mask for patterning parylene over the electrode pattern. The holes below either ends of the contact pads (Figure 3.2(B)) are used for aligning the SEI interface connector with the contact pads. The two alignment pins of the SEI connector go into each of the holes.

The PerFlexMEA being extremely fragile was reinforced with Kapton tape at the edges and at the region around the alignment holes. This prevented the membrane from tearing during handling. The bottom surface of the membrane near the contact pads was

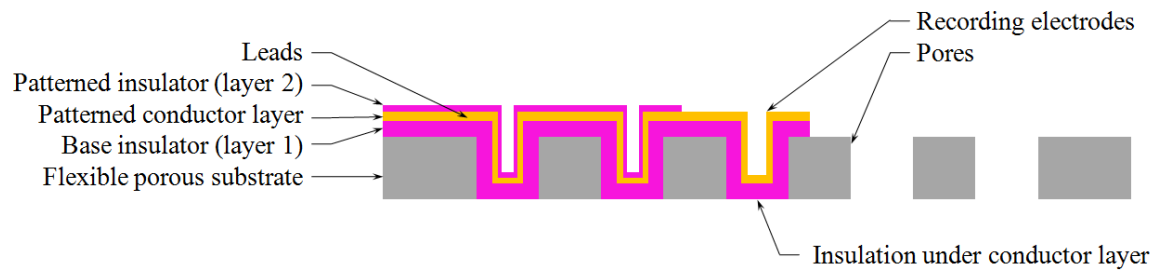


Figure 3.3 Layer architecture of PerFlexMEA. Cross-sectional view of a lead and electrode region. Parylene completely blocks the conductor layer from the bottom (layer 1) and only the leads at the top (layer 2).

further sealed with Kapton tape to further insulate and prevent wetting the contact pads from the bottom.

### 3.3 Layer Architecture

The device required deposition and patterning of three layers on the flexible polycarbonate substrate. Two of the layers acted as insulators (parylene – layer 1 and 2) and sandwiched the conduction layer (gold over titanium oxide over titanium) between them. Figure 3.3 illustrates the basic layer architecture.

#### 3.3.1 Parylene (Layer 1)

Parylene formed the bottommost layer (approximate layer thickness = 500 nm). It blocked the pores below the patterned regions, insulating the conducting leads and electrodes from the bottom.

### 3.3.2 Gold

Gold was deposited over the first parylene layer and formed the conducting layer (approximate layer thickness = 100 nm). A thin layer of titanium/titanium dioxide was deposited before gold to augment adhesion to parylene.

### 3.3.3 Parylene (Layer 2)

Parylene is the topmost layer (approximate layer thickness = 500 nm). It is patterned to cover the leads of the patterned conductor layer. This layer is not deposited over the recording electrodes and contact pads.

### 3.4 References

- [1] *Corning Incorporated*. Available: [www.corning.com](http://www.corning.com)
- [2] B. E. Isakson and B. R. Duling, "Heterocellular contact at the myoendothelial junction influences gap junction organization.," *Circ Res*, vol. 97, pp. 44-51, Jul 2005.
- [3] G. S. Goldberg, A. P. Moreno, and P. D. Lampe, "Gap junctions between cells expressing connexin 43 or 32 show inverse permselectivity to adenosine and ATP.," *J Biol Chem*, vol. 277, pp. 36725-30, Sep 2002.
- [4] *Sterlitech Corporation*. Available: [www.sterlitech.com](http://www.sterlitech.com)
- [5] *Samtec Inc*. Available: [www.samtec.com](http://www.samtec.com)
- [6] S. A. Boppart, B. C. Wheeler, and C. S. Wallace, "A flexible perforated microelectrode array for extended neural recordings," *IEEE Trans Biomed Eng*, vol. 39, pp. 37-42, Jan 1992.
- [7] C. González and M. Rodríguez, "A flexible perforated microelectrode array probe for action potential recording in nerve and muscle tissues.," *J Neurosci Methods*, vol. 72, pp. 189-95, Apr 1997.
- [8] B. A. Hollenberg, C. D. Richards, R. Richards, D. F. Bahr, and D. M. Rector, "A MEMS fabricated flexible electrode array for recording surface field potentials," *J Neurosci Methods*, vol. 153, pp. 147-53, May 15 2006.
- [9] D. P. O'Brien, T. R. Nichols, and M. G. Allen, "Flexible microelectrode arrays with integrated insertion devices," presented at the The 14th IEEE International Conference on Micro Electro Mechanical Systems, Interlaken, 2001.
- [10] P. J. Rousche, D. S. Pellinen, D. P. Pivin, Jr., J. C. Williams, R. J. Vetter, and D. R. Kipke, "Flexible polyimide-based intracortical electrode arrays with bioactive capability," *IEEE Trans Biomed Eng*, vol. 48, pp. 361-71, Mar 2001.
- [11] J. M. Hsu, L. Rieth, R. A. Normann, P. Tathireddy, and F. Solzbacher, "Encapsulation of an integrated neural interface device with Parylene C.," *IEEE Trans Biomed Eng*, vol. 56, pp. 23-9, Jan 2009.
- [12] G. E. Loeb, M. J. Bak, M. Salcman, and E. M. Schmidt, "Parylene as a chronically stable, reproducible microelectrode insulator.," *IEEE Trans Biomed Eng*, vol. 24, pp. 121-8, Mar 1977.
- [13] D. Rodger, A. Fong, L. Wen, H. Ameri, A. Ahuja, C. Gutierrez, I. Lavrov, Z. Hui, P. Menon, E. Meng, J. Burdick, R. Roy, V. Edgerton, J. Weiland, M. Humayun, and Y. Tai, "Flexible parylene-based multielectrode array technology for high-density neural stimulation and recording," *SENSORS AND ACTUATORS B-CHEMICAL*, pp. 449-460, JUN 16 2008 2008.

## CHAPTER 4

### FABRICATION

The MEA device was fabricated in clean room environment at the Nanofab laboratories, University of Utah. The electrode array was developed on one side of a PCTE membrane. Fabrication of the PerFlexMEA presented three major challenges.

- (1) *Fabrication on a flexible substrate* – Lithography and anisotropic etching requires the substrate to be maintained flat. Furthermore, in lithography, a rigid substrate is desirable during UV exposure through the mask. To accurately transfer the mask pattern onto the substrate, the mask and substrate have to be held tightly against each other. A slightest gap between the two might reduce the feature size.
- (2) *Insulation of gold from bottom* – The gold electrodes and leads would record from the cells on the opposite side of the membrane through the pores. The conduction layer needs to be blocked from the bottom to avoid recording from the cells on the other side of the membrane.
- (3) *Recovering porosity of selected regions of substrate* – Some of the deposition processes are isotropic and might block the membrane pores. Appropriate deposition and etching processes would be needed to restore the porosity of the membrane at the required regions (cell culture zone).

The next section describes and discusses the methods engineered to overcome these problems.

## 4.1 Microfabrication Process

### 4.1.1 Membrane Adhesion to Rigid Substrate

Since some of the microfabrication processes involved are isotropic and some require the substrate to be rigid, the flexible membrane had to be maintained flat throughout the fabrication process. The PCTE membrane was adhered to a rigid glass slide, thus obtaining a rigid substrate. Furthermore, to block the membrane pores from the bottom, a thick photoresist was selected to adhere the membrane to the glass slide. AZ 4620 photoresist had the appropriate viscosity for attaching the membrane to the rigid substrate and blocking the pores from the bottom. A glass slide with a clean surface was selected (Figure 4.1(A)). AZ 4620 photoresist was spun on the glass slide at 2500 rpm for 50 s to form an 8-10  $\mu\text{m}$  thick photoresist layer (Figure 4.1(B)). The resulting wafer was then baked at 90 °C for 5 minutes on a hot plate to give the photoresist a smooth and uniform surface. The PCTE membrane was cut appropriately and placed flat on the photoresist surface using tweezers (Figure 4.1(C)). The wafer with the membrane was baked further, which stretched the membrane, generating bubble-like wrinkles on the membrane (Figure 4.2(A)). These wrinkles were wiped gently with the finger towards the edges of the membrane. Most of the formed wrinkles were wiped off in about 3-4 minutes, after which the wafer was cooled (Figure 4.2(B)). Binding the membrane to a glass substrate provides a rigid substrate ideal for lithography and blocks the pores in the membrane, restricting coating only on one side of the membrane.

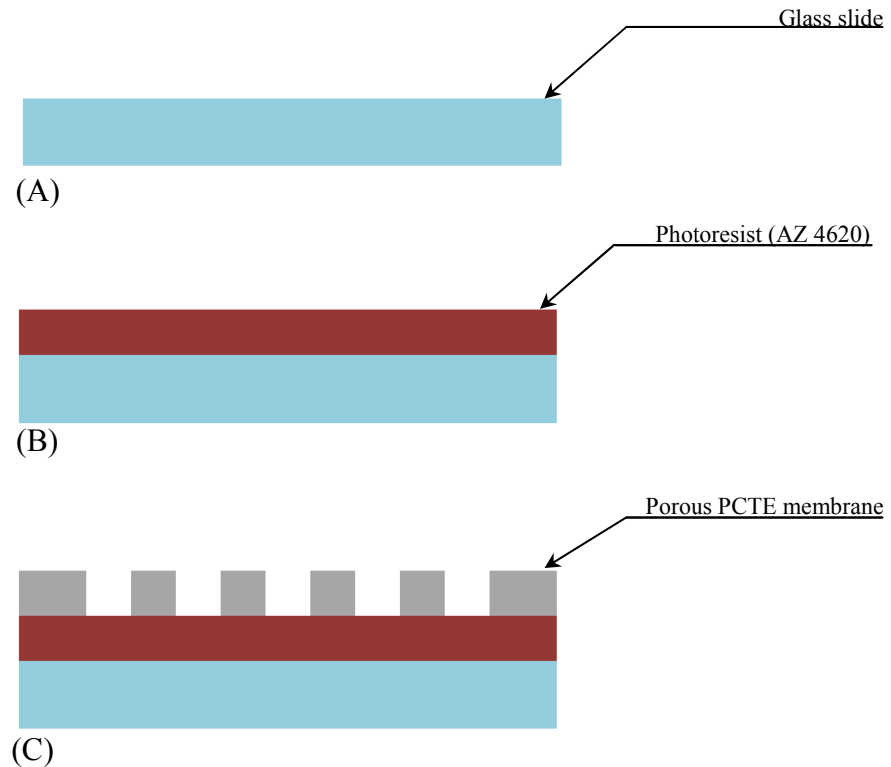


Figure 4.1 Fabrication steps 1 to 3 - (A) Clean rigid glass substrate for adhering the flexible membrane. (B) 8-10  $\mu\text{m}$  layer of AZ4620 spin-coated onto the glass substrate. AZ4620 is used as an adhesive and for blocking the membrane pores from the bottom. (C) Porous and flexible PCTE membrane adhered to the rigid glass substrate. The pores are blocked at the bottom.

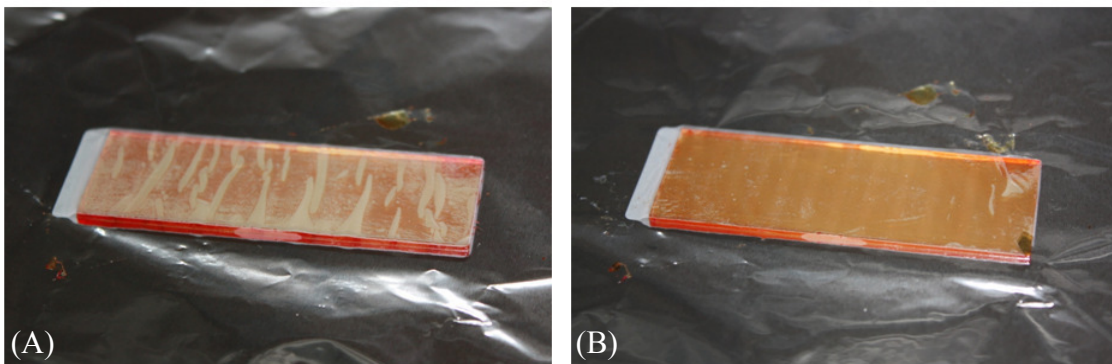


Figure 4.2 Membrane adhesion process. The glass substrate is kept on a hot plate at 90  $^{\circ}\text{C}$ . (A) The membrane forms wrinkles after baking approximately 1 minute (B) Further baking (3-4 minutes) and gently rubbing removes the wrinkles and bubbles, flattening the membrane and making it adhere to the photoresist (AZ4620) layer.

#### 4.1.2 Parylene Deposition – Layer 1

The membrane was then coated with parylene<sup>1</sup> by a low pressure vapor deposition process (LPCVD) which consumed 0.9 grams of parylene dimer to produce a 460 nm thick parylene coating (layer 1) on all exposed surfaces including the walls of the pores, as shown in Figure 4.3. Coating the membrane using an isotropic process blocks all the pores at the bottom. Therefore, any other layer deposited (conductor layer) on this will be insulated from the bottom surface of the membrane.

#### 4.1.3 Pre-Etch to Promote Metal Adhesion

The parylene layer was dry etched<sup>2</sup> for 30 s using oxygen as the etching gas (Figure 4.4). Etching roughens the top parylene surface and improves adhesion of metal layers deposited on it [1].

#### 4.1.4 Metal Deposition

A multicathode sputtering system<sup>3</sup> was used to deposit titanium (Ti), titanium dioxide (TiO<sub>2</sub>), followed by gold (Au) over the parylene surface (Figure 4.5). The deposited metal layers measured an average total thickness of 130 nm. While gold works as the principle conductor, titanium and titanium oxide augments gold adhesion to parylene. Figure 4.6 shows the sputtered gold surface.

---

<sup>1</sup> Parylene coating done using PDS 2010 parylene coater (Specialty Coating Systems<sup>TM</sup>, Indianapolis, USA)

<sup>2</sup> Dry etching done using Plasmalab 80 Plus system (Oxford Instruments, Oxfordshire, UK)

<sup>3</sup> Sputtering done using SS-40C-IV, Multicathode sputtering system (T-M Vacuum Products, Inc., Cinnaminson, USA)



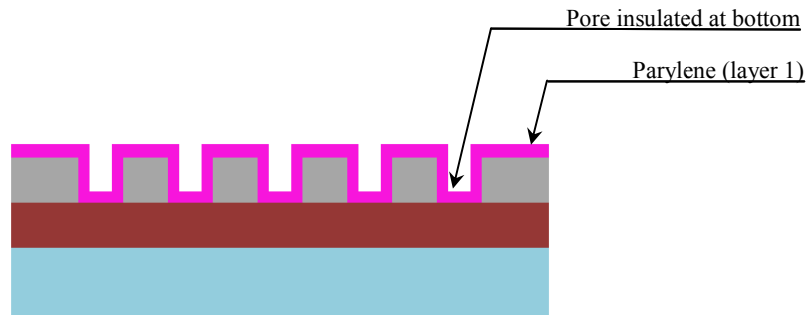


Figure 4.3 Parylene coating by LPCVD process. The deposition process is isotropic which results in a uniform coat of parylene layer on all exposed surfaces. This includes the pore sidewalls and the exposed photoresist surface beneath the membrane.

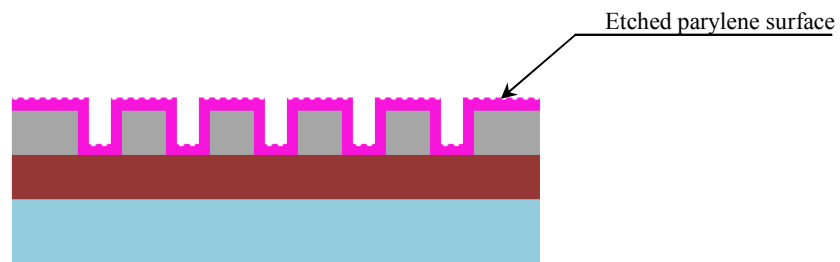


Figure 4.4 Reactive ion etching of parylene surface. Etching the surface for 30 s coarsens the parylene surface. A courser surface promotes metal adhesion.

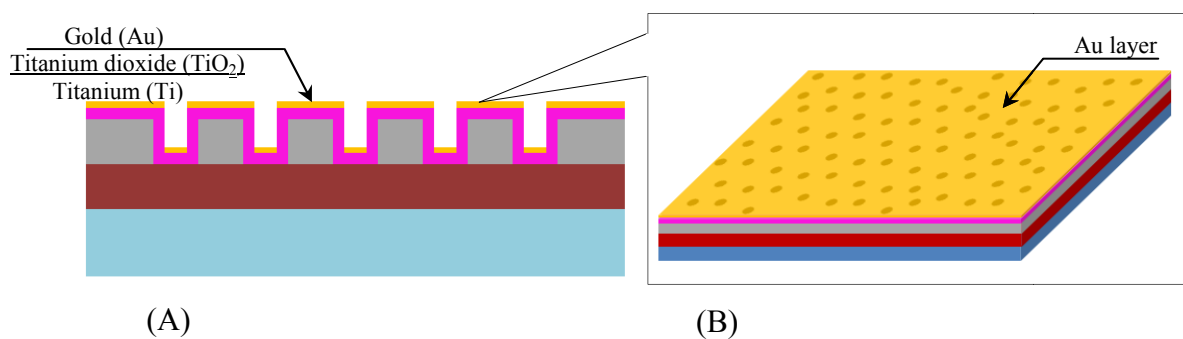


Figure 4.5 Conductor layer deposition by sputtering. (A) Metals (and metal oxide) were deposited over parylene in the following order – Titanium, titanium dioxide and gold. Titanium and titanium dioxide promote gold (topmost layer) adhesion. Since, the deposition process was anisotropic, the pore sidewalls were not coated. (B) View of the top surface coated with gold.

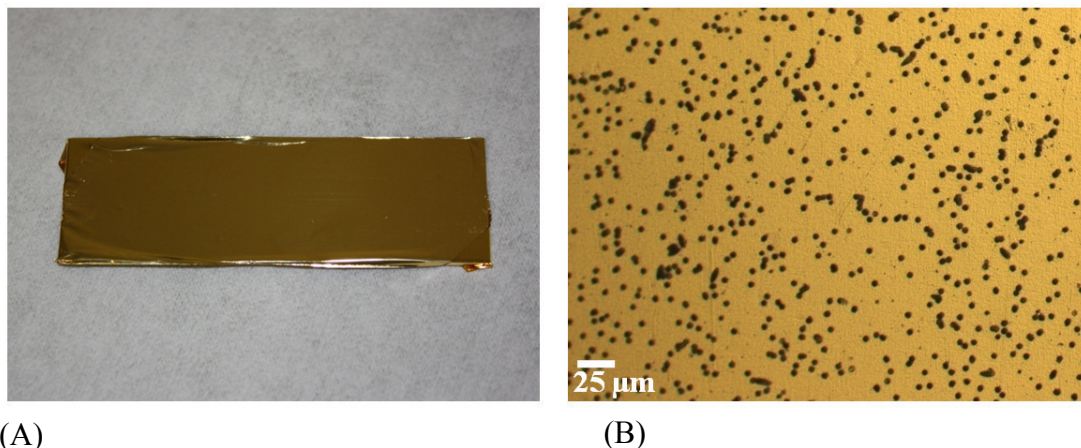


Figure 4.6 Sputtered gold surface (A) Photograph of the glass slide with the gold deposited membrane. (B) Magnified photograph (at 10x magnification) of the gold coated surface on the membrane. The black dots are the pores.

#### 4.1.5 Mask Generation for Lithography

The electrode and insulator patterns were designed using L-Edit CAD software<sup>4</sup>. The pattern designs for the conductor layer (Figure 4.7(A)) and insulator layer (Figure 4.7(B)) were printed on a 5 inch (12.7 cm) square glass plate<sup>5</sup>. The mask was then oven-baked at 115 °C for 20 minutes. It was cooled for 2-3 minutes and placed in a glass container. AZ 300 MIF was poured slowly to cover the complete mask and left for 10 s. At the end of 10 s the mask was quickly removed and washed in DI rinse (high rinse). The designed patterns became visible on a shiny background. The mask was then dipped in Cr 14-S chromium etch for 4.5 to 5 minutes until the mask becomes transparent, leaving behind the pattern on the glass. The mask was then washed in DI rinse and dried.

<sup>4</sup> Tanner EDA, Los Angeles, USA

<sup>5</sup> Mask was printed using the Electromask MM250 pattern generator (Interserv Technology, New Brighton, USA)

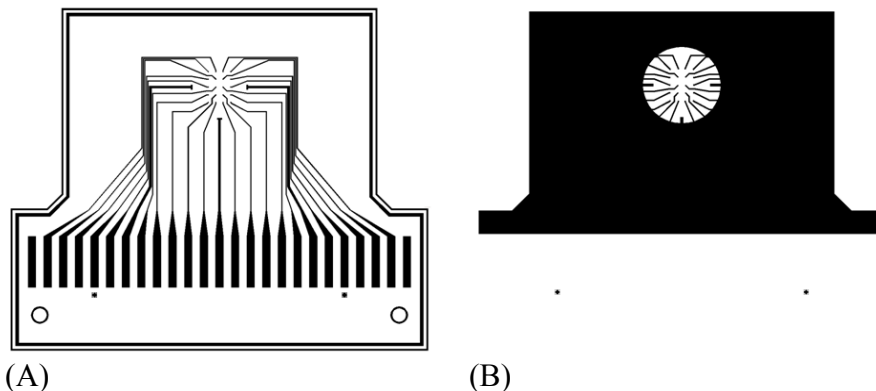


Figure 4.7 Mask patterns. Two separate mask patterns were developed on a 5 inch glass plate for lithography. (A) Mask pattern for conductor layer (gold + titanium + titanium dioxide). (B) Mask pattern for parylene layer (layer 1 + layer 2).

#### 4.1.6 Gold Patterning

Lithography was used to pattern the metal/conducting layer comprising of the electrodes, leads and contact pads. The wafer was spin coated with photoresist (Shipli 1813) at 3000 rpm for 10 s and baked at 90 °C for 6 minutes. The photoresist layer was then exposed to Ultra Violet (UV) light for 8 s through the mask (Figure 4.7(A)). The mask blocked the UV light, exposing only the nonshaded regions of the mask. The wafer was then washed in developer 352 solution for 50 s until the exposed photoresist dissolved. The wafer with the remaining photoresist pattern was washed in DI rinse (deionised water rinse), dried, postbaked and exposed to UV light for another 8 s (Figure 4.8). Since gold was shielding the photoresist at the bottom layer, only the patterned photoresist layer got exposed. The wafer was then washed in KI/I<sub>2</sub> solution for about 30 s which removed the uncovered gold. The wafer was washed in DI rinse, dipped in Buffered Oxide Etch (BOE) solution for 10 s and again washed in DI rinse. The BOE solution selectively etches the titanium and titanium dioxide layer. Once the electrodes were patterned, the solution was washed in developer 352 for 50 s to remove the

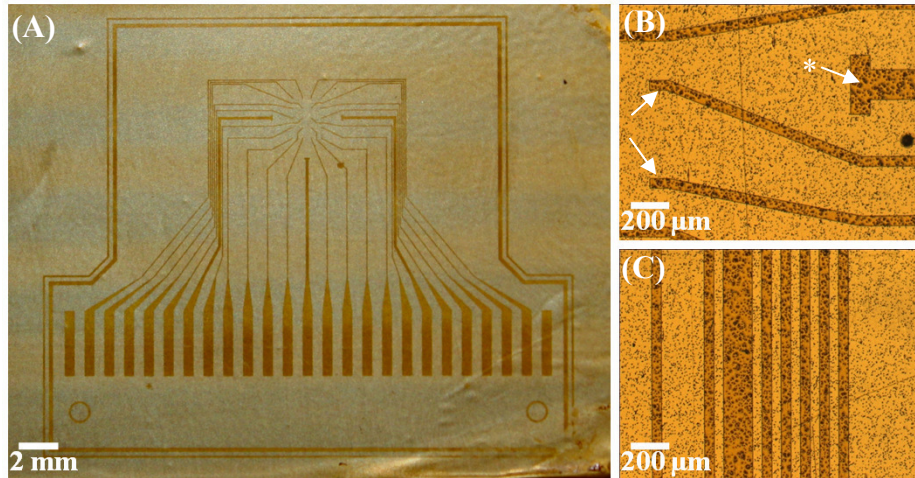


Figure 4.8 Photoresist pattern transferred on metal layer by lithography for patterning metal layer. (A) Photograph of the entire photoresist pattern formed for the metal layer. (B) A magnified view (5x) of the photoresist pattern showing a few electrodes and a stimulating electrode\*. (C) Photoresist pattern of the leads. The thick lead connects the stimulating electrode.

remaining patterned photoresist (Figure 4.9). Figure 4.10 shows photographs of the patterned conductor layer.

#### 4.1.7 Parylene Deposition – Layer 2

Parylene was again deposited<sup>2</sup> using 0.9 grams of dimer to obtain the second coat (shown in Figure 4.11 as the translucent pink layer). The same LPCVD method used in Section 4.1.2 was utilized and a 510 nm thick parylene coat was obtained.

#### 4.1.8 Parylene Patterning

Patterning of the entire parylene layer (layer 1 + layer 2) was done by lithography as explained in Section 4.6, but with a different mask (Figure 4.7(B)) and an additional alignment step with the existing gold pattern on the wafer.

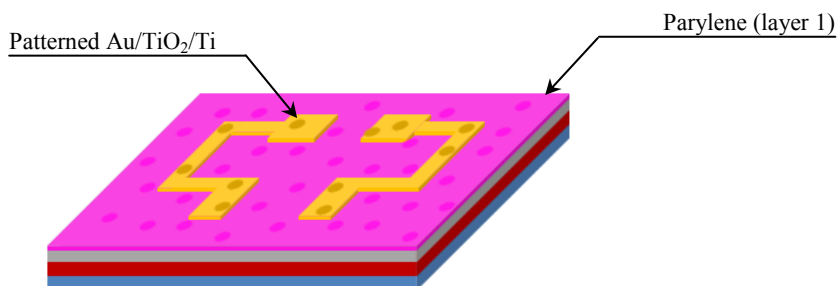


Figure 4.9 Patterning of metal layers by lithography and wet etching. The yellow regions indicate the result of patterning gold by wet etching using  $\text{KI/I}_2$  solution and  $\text{TiO}_2/\text{Ti}$  with buffered oxide etch (BOE).

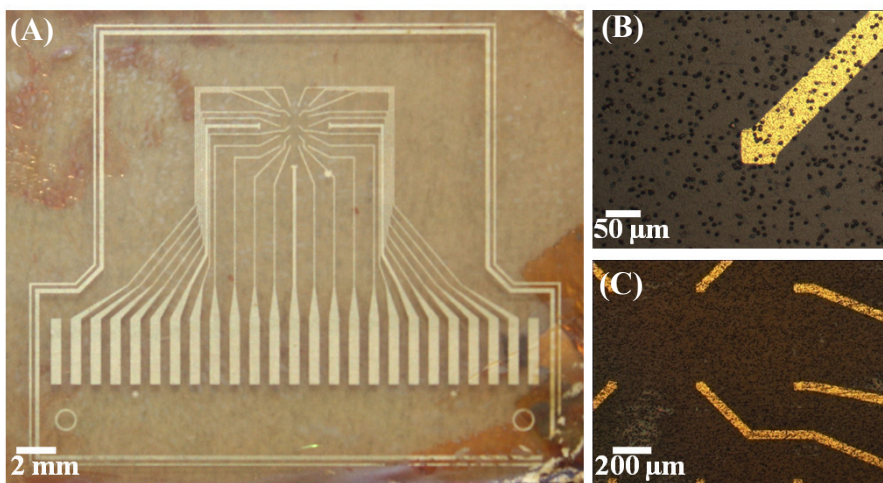


Figure 4.10 Patterned metal layers after wet etching with  $\text{KI/I}_2$  and BOE solution. (A) Photograph of the patterned metal layer on the membrane. The substrate appears transparent. (B) Magnified view (20x) of a single square recording electrode with its lead. (C) Patterned electrodes with their respective leads in the cell culture zone.

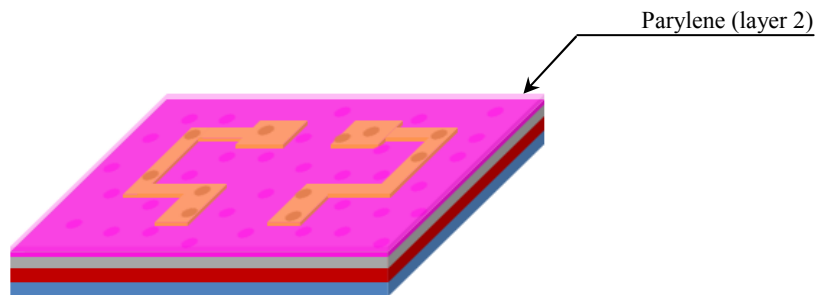


Figure 4.11 Parylene coat (layer 2) covering the patterned metal layer. The second parylene layer was deposited using LPCVD process. The parylene insulated (translucent pink) the patterned metal layer (seen in yellow) from the top.

Once aligned<sup>6</sup>, the photoresist layer was exposed to UV light for 8 s, washed in developer 352 to dissolve the exposed photoresist, followed by a DI rinse and drying (Figure 4.12). The wafer was then etched implementing an anisotropic process – reactive ion etching (RIE) – in the Plasmalab 80. RIE was carried out for 7 minutes to remove the uncovered parylene layer (layer 1 + layer 2), leaving the final parylene pattern (Figure 4.13).

#### 4.1.9 Cutting and Reinforcement of Alignment Holes

Each device on the membrane was reinforced with Kapton tape as shown in Figure 4.14. Once reinforced, the alignment holes were cut using a punch followed by the edges of the device. Cutting out the membrane was much simpler while adhered to a rigid substrate. Furthermore, it also condensed the exfoliation process by reducing the area of membrane to be peeled off.

<sup>6</sup> Mask-wafer alignment was done using an EVG 420 mask aligner (Electronic Vision Group, St. Florian Am Inn, Austria)

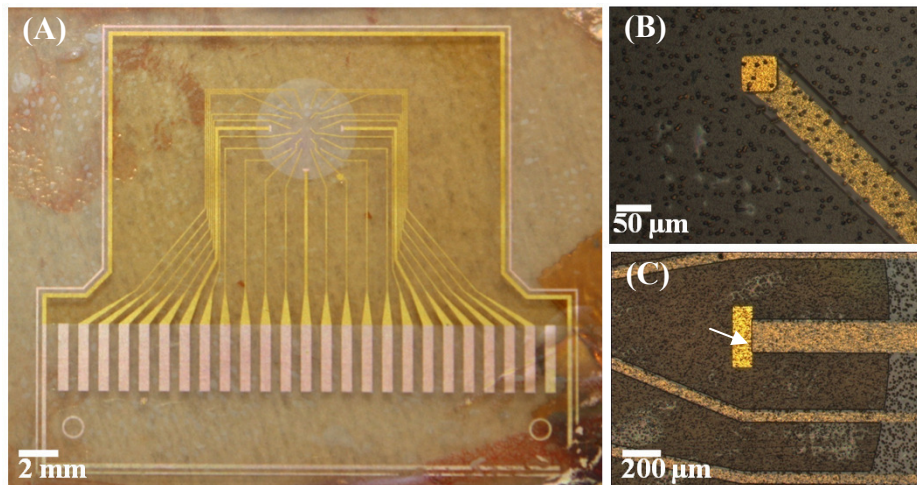


Figure 4.12 Photos resist pattern for parylene patterning. (A) Photograph of the entire photos resist pattern on the parylene layer. (B) Magnified view (20x) of an electrode with its lead covered with photos resist. The photos resist cover is slightly wider (10  $\mu\text{m}$  on each side) than the electrode leads. This ensures complete insulation of leads. (C) Magnified view (5x) of a stimulating electrode with its lead covered with photos resist.

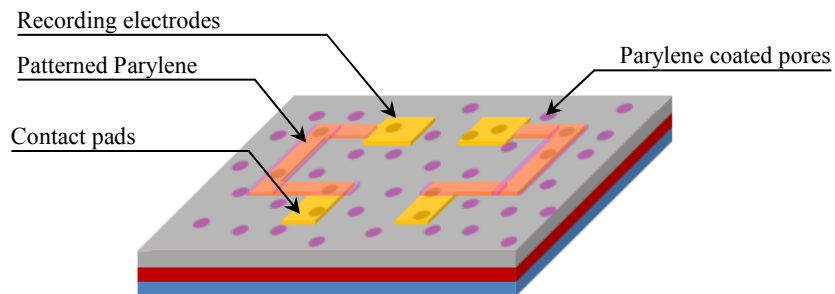


Figure 4.13 Parylene patterning. After patterning, the parylene from the recording electrodes and contact pads are etched, exposing them. The leads are insulated by parylene at the top and bottom, whereas the electrodes and contact pads are insulated only at the bottom. The parylene pores' sidewalls are not removed as the RIE process is anisotropic.

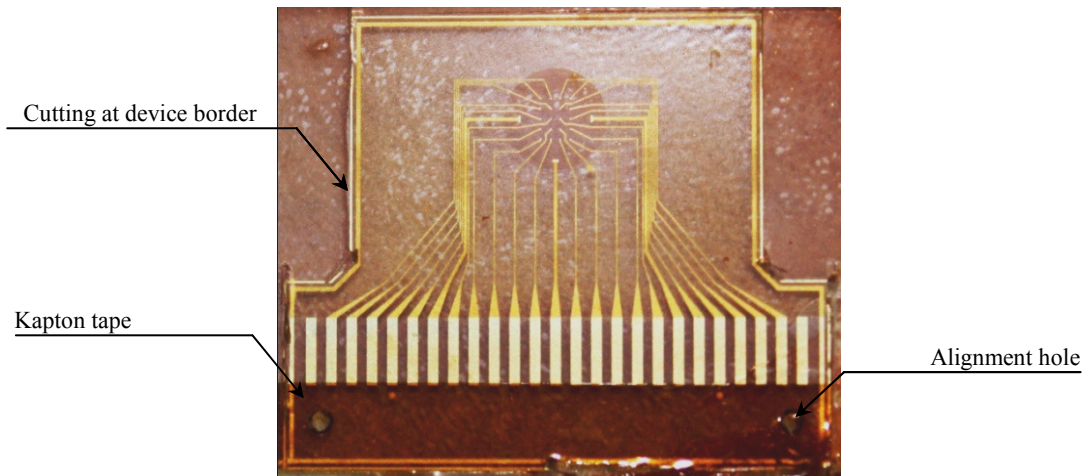


Figure 4.14 Membrane reinforcement and cutting. The Kapton tape was attached to the membrane at the end covering the alignment holes and leaving the contact pads exposed. The alignment holes were cut after taping the membrane's end. The membrane was cut around the device borders (patterned gold).

#### 4.1.10 Exfoliation from Rigid Glass Substrate

The wafer was then soaked in AZ400K solution with gentle stirring to peel off the newly formed PerFlexMEA. It took around 25 minutes for the AZ400K solution to soak the porous sections of the membrane (Figure 4.15). The darkening of the recording zone (Figure 4.15(C)) in the device confirms porosity at the desired region. Once the membrane came off, it was washed in DI rinse and dried (Figure 4.16).

The PerFlexMEA was handled using forceps and stored in a 35mm Petri dish. The edges and bottom of the contact pads were further reinforced with Kapton tape. The PerFlexMEA was washed with PBS and ethanol, followed by an autoclaving process to sterilize it before cell culture.



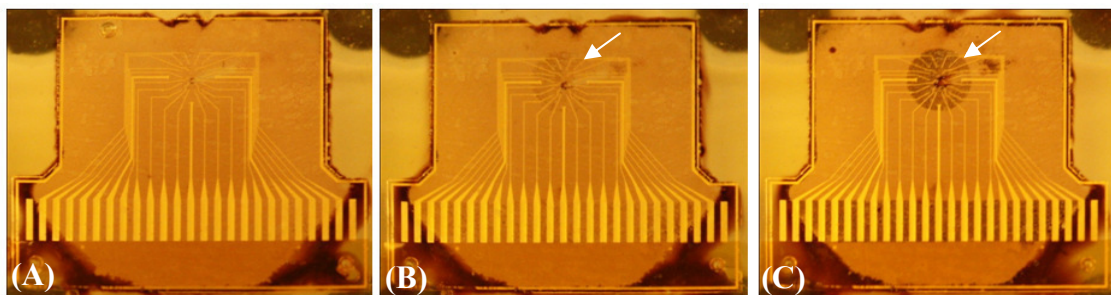


Figure 4.15 Soaking of substrate in AZ400K. The glass substrate with the membrane was soaked in AZ400K for exfoliating the patterned device. A to C show a sequence of photographs of the device immersed in the solution (A) after 1 minute (B) after 10 minutes (C) after 25 minutes. AZ400K dissolves the AZ4260 (photoresist) and can be identified as a dark red/maroon color. Note that with time, AZ400K permeates through the pores at the circular cell culture zone (arrows) and reacts with AZ4620. This results in a dark red/maroon area in C.

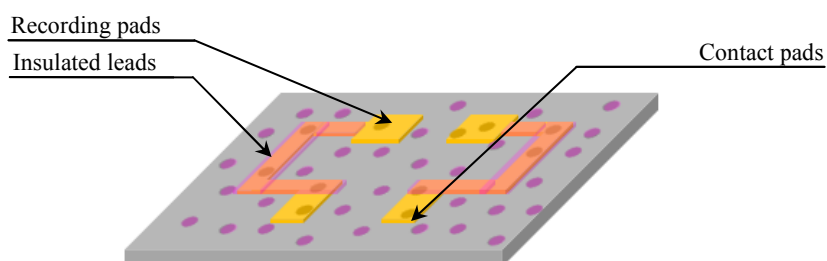


Figure 4.16 The PerFlexMEA after exfoliation. The patterned device is free from the AZ4620 and rigid substrate that held it at the bottom.

## 4.2 Characterization

### 4.2.1 Layer Thickness

Since the main polycarbonate substrate is extremely fragile, deposition thickness measurements were not conducted directly to avoid damaging the device during measurement. Separate glass slides were placed along with the substrate during coating processes. The reported layer thicknesses have been measured on the sample glass slides. For each of the layers, the thickness was measured at five different points.

Polycarbonate membrane thickness = 9  $\mu\text{m}$

Parylene layer 1 thickness = 460  $\pm$  10 nm

Electrode layer thickness = 130  $\pm$  10 nm

Parylene layer 2 thickness = 510  $\pm$  10 nm

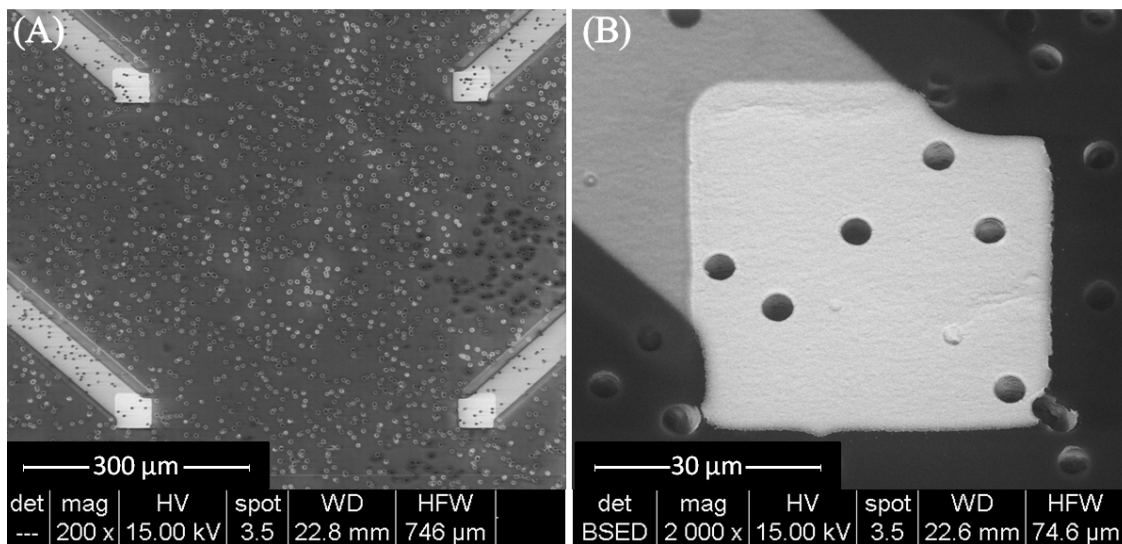


Figure 4.17 SEM images of the patterned gold electrodes and parylene on the polycarbonate membrane at different magnifications. (A) Four patterned recording electrodes with parylene covered leads (at 200x magnification). (B) Close up of a single recording electrode pad (at 2000x magnification).

#### 4.2.2 Electrode Resistance

The PerFlexMEA was adhered to a glass slide using Kapton tape for measuring electrode resistances. The device was setup in a probe station<sup>7</sup> with one probe tip at the recording electrode and the other probe tip at its corresponding contact pad. The probes were connected to a Keithley 4200 semiconductor parameter analyzer<sup>8</sup>. Figure 4.18 shows the measured electrode and stimulator resistance values.

The values marked N/A could not be measured due to electrode damage during measurement. Since the device was symmetrically designed about the central stimulator, the electrode resistance values were the same as their corresponding symmetric positions. The resistance values ranged from 129  $\Omega$  to 230  $\Omega$ . The main cause of this wide range was the variation in lead lengths.

---

<sup>7</sup> Cascade Microtech Inc., Beaverton, USA

<sup>8</sup> Keithley Instruments Inc., Cleveland, USA

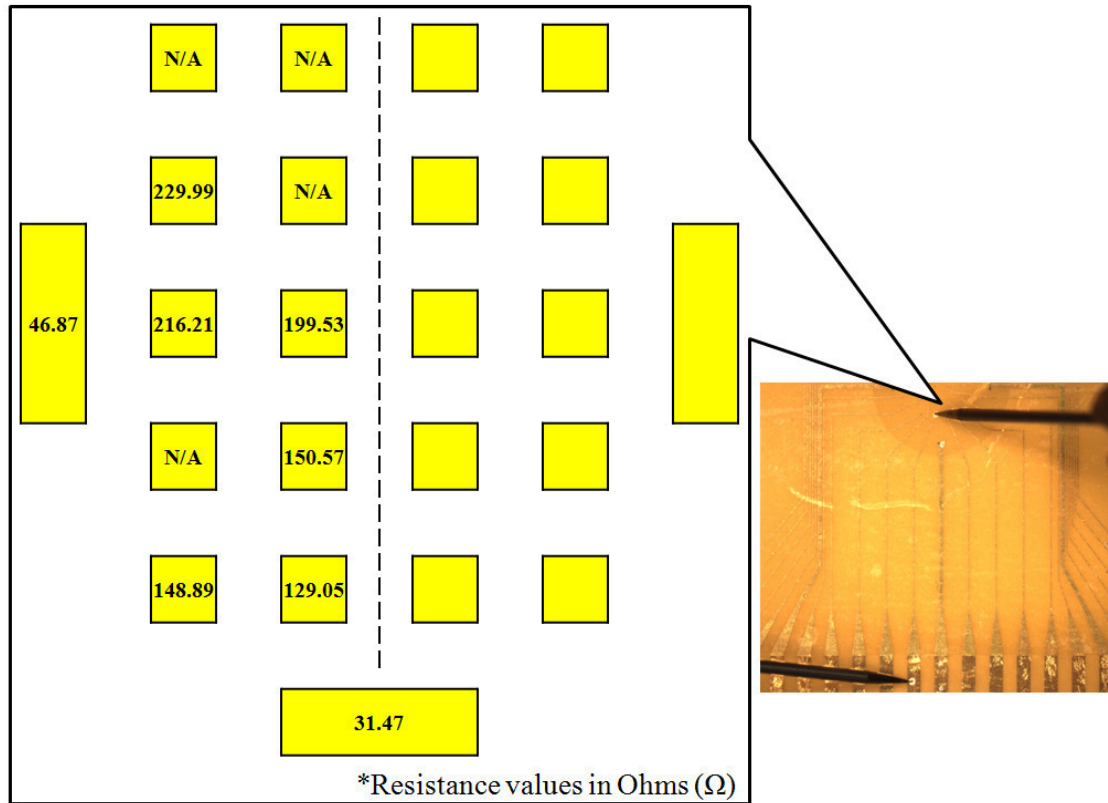


Figure 4.18 Resistance measurements of recording and stimulating electrodes. In the dialogue box, the yellow colored squares represent the recording electrodes and rectangles represent the stimulating electrodes, arranged as in the PerFlexMEA. The resistance values between the recording/stimulating electrodes and their corresponding contact pads are indicated (measured in  $\Omega$ ). The squares labeled N/A were from the recording electrodes whose resistances could not be measured due to electrode damage during recording. The blank squares/rectangles have the same resistances as the symmetrically positioned electrodes about the dashed line at the centre.

### 4.3 References

- [1] J. W. Seonga, K. W. Kimb, Y. W. Beagb, S. K. Kohb, K. H. Yoonc, and J. H. Leec, "Effects of ion bombardment with reactive gas environment on adhesion of Au films to Parylene C film," *Thin Solid Films*, vol. 476, pp. 386-390, 8 April 2005 2005.

## CHAPTER 5

### PACKAGING AND INTERFACE

The fabricated membrane was delicate and especially prone to tearing during handling. To make the PerFlexMEA easier to handle, a protective housing had to be developed. A coin setup was designed and fabricated for packaging and interfacing to the PerFlexMEA. The coin setup accomplishes the following three functions:

- (1) *Membrane handling* – Since the membrane was vulnerable to tearing easily during handling, a protecting housing device was imperative. Furthermore, the flexible membrane had to be maintained flat for culturing the cells onto it.
- (2) *Isolating cell culture zone* – The region where cells were cultured needed to be maintained under solution, whereas the contact pads needed to be maintained dry to avoid short circuits and signal duplication.
- (3) *Interfacing amplifier system to recording electrodes* – Since the substrate (PCTE membrane) was quite fragile, an appropriate contact mechanism had to be selected. A 25-pin commercially available coiled connector was used and appropriately assembled into the coin. Figure 5.1 shows the selected SEI connector aligned to the contact pads of the PerFlexMEA.

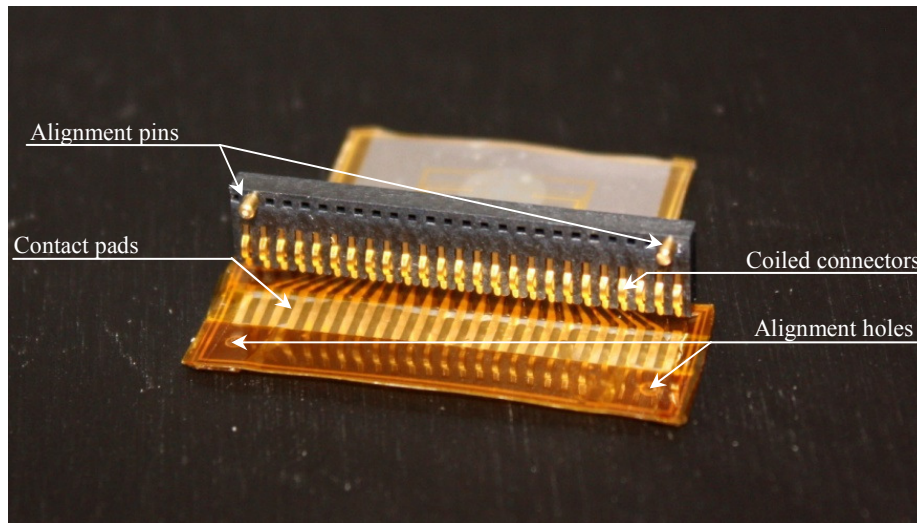


Figure 5.1 Samtec SEI connector<sup>1</sup> aligned to the PerFlexMEA contact pads. The two alignment pins on the SEI connectors correspond to the holes on the Kapton tape of the PerFlexMEA which align the coiled connectors to their corresponding contact pads.

### 5.1 The Coin Setup

The coin setup was developed taking into consideration the following design constraints:

- (1) *Material* – The selected materials not only had to be biocompatible but also be able to withstand temperatures up to 200 °C. The complete device was required to be autoclaved before each use, where the device was subjected to temperatures up to 200 °C.
- (2) *Standard culture Petri dish (60mm)* – The packaging and interfacing setup had to fit in a standard Petri dish. This simplified the maintenance of the cultured preparation as the whole setup could be immersed in media held in the 60 mm dish. This restricted the size of the coin setup to Ø57 mm × H10 mm.

---

<sup>1</sup> Samtec Inc., New Albany, USA

(3) *Samtec SEI connector (25 pin)* – To interface with the PerFlexMEA, a suitable contact mechanism had to be chosen that would not damage the thin flexible PCTE membrane and at the same time be able to maintain proper contact with the contact pads. The Samtec 25-pin SEI connector (one piece interface) was selected to interface with the contact pads on the PerFlexMEA. Its coiled connector structure ensured proper contact without damaging the flexible membrane. The SEI connector needed a housing system for maintaining it dry. The size (L35.25 mm × B6.1 mm × H2 mm) restricted its position in the coin and the minimum designable coin height.

(4) *Fasteners (Ø2.2 mm)* – The use of the coiled connectors as interface and to isolate the electronic interface part using an elastomer layer required the elastomer layer to be held tightly between the rigid PCTFE plates. A tight seal between the plates and the elastomer layer was imperative in keeping the electronic interface region dry. Fasteners presented the most compact and reliable method for tightly holding the different layers together. Ø2.2 mm fasteners were selected to ensure tight packing of the coin setup. In order to allow tight fastening, appropriate material thickness had to be maintained to avoid material failure. This added about 2 mm height (or thickness) on each side of the fastener (nut and screw head).

Based on the discussed design constraints, materials were selected and a coin setup was designed. The coin setup was fabricated using PCTFE (polychlorotrifluoroethylene)—a validated biocompatible polymer—and manufactured to highly precise specifications. The fabricated ensemble of pieces when assembled was able to align and hold the PerFlexMEA and properly connect its gold contact pads with



the recording system using a SEI one piece interface with coiled connectors. The coin was designed to fit inside a 60 mm plastic Petri dish where cells could be cultured and maintained inside a CO<sub>2</sub> incubator.

The coin could be functionally divided into two parts (as shown in Figure 5.2(C)):-

- (1) *Cell culture and recording part* – This constituted the front half of the coin where the membrane electrodes were positioned. Cells could be cultured and maintained.
- (2) *Electronic interface part* – This constituted the back half (with the flat end) which formed the junction for connecting the amplifier system to the recording electrodes at the membrane contact pads via the SEI connectors.

Figure 5.3 shows the main parts of the coin in an exploded view. The parts involved were designed to form 3 layers. The bottom plate had an oblong hole that acted as the bottom half of the culture chamber and a 10 µm depression for PerFlexMEA positioning and alignment. The top back plate held the selected connectors that were aligned with the contact pads of the PerFlexMEA.

A 25-pin, 1 mm pitch, SEI series, one piece interface was used to connect the contact pads on the PerFlexMEA to the amplification and recording system. The SEI contacts were surrounded by a layer of Sylgard® 184 silicone elastomer<sup>2</sup>. This layer was sandwiched tightly by the top and bottom plates to seal the region around the SEI contacts and membrane contact pads, keeping them dry. The top front plate contains a hole that acts as the top half of the culture chamber. The cell culture zone was also surrounded by a Sylgard® layer to avoid leaking of cells during plating. Two rounded rectangular alignment pins were provided to align the top front plate and the Sylgard®

---

<sup>2</sup> Dow Corning Corp., Midland, USA

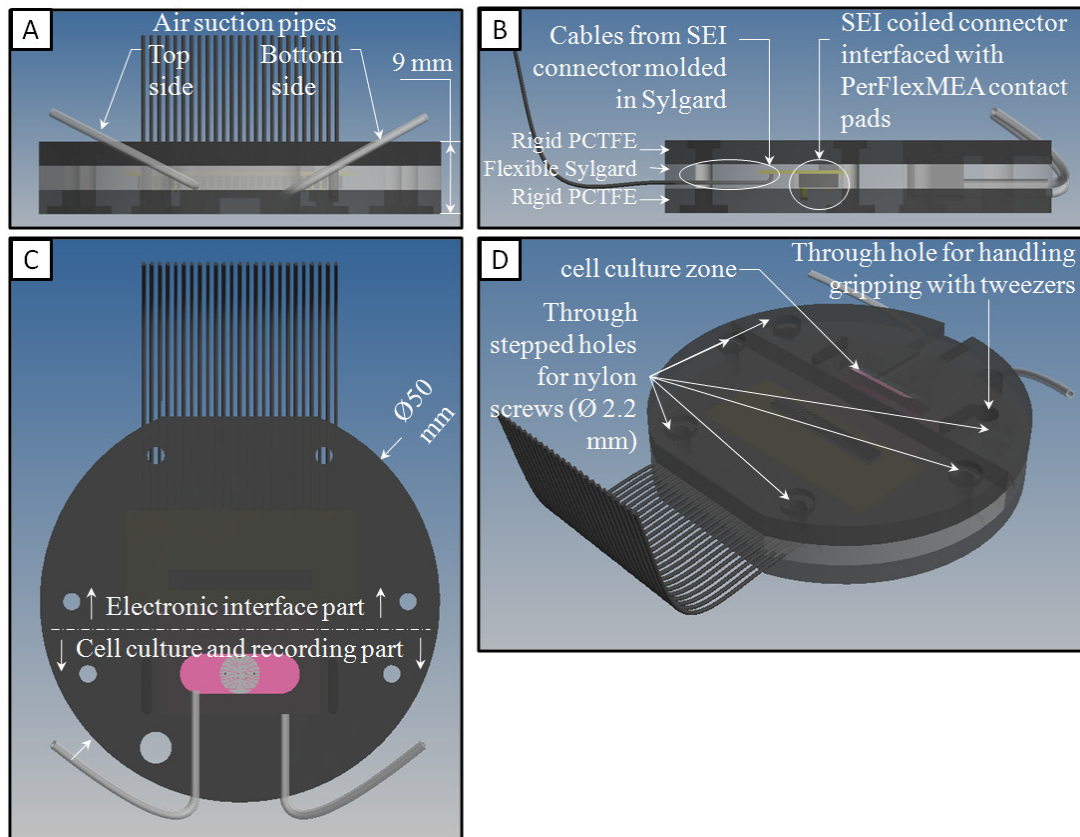


Figure 5.2 Assembled coin setup for housing the PerFlexMEA. The different views show some of the key dimension and design features of the coin setup. (A) Front view. (B) Side view. (C) Top view and (D) isometric view. The coin setup was designed to fit in a 60 mm Petri dish. Views were produced using Autodesk Inventor Professional 2011.

layer to the bottom plate during assembly. Two air suction pipes were positioned on each side of the membrane to suck out any air bubbles trapped in the membrane side facing down. Two channels are provided to each side of the culture zone to allow media movement. All pieces were secured together using 6 nylon screws (not shown in Figure 5.2 and 5.3). The cables from the SEI connector were molded in the Sylgard® and came out from the flat end of the coin (Figure 5.4). The 20 recording cables were connected to a standard 20-pin female flat ribbon connector. The 3 stimulator pin cables were connected to a 3 pin female connector.

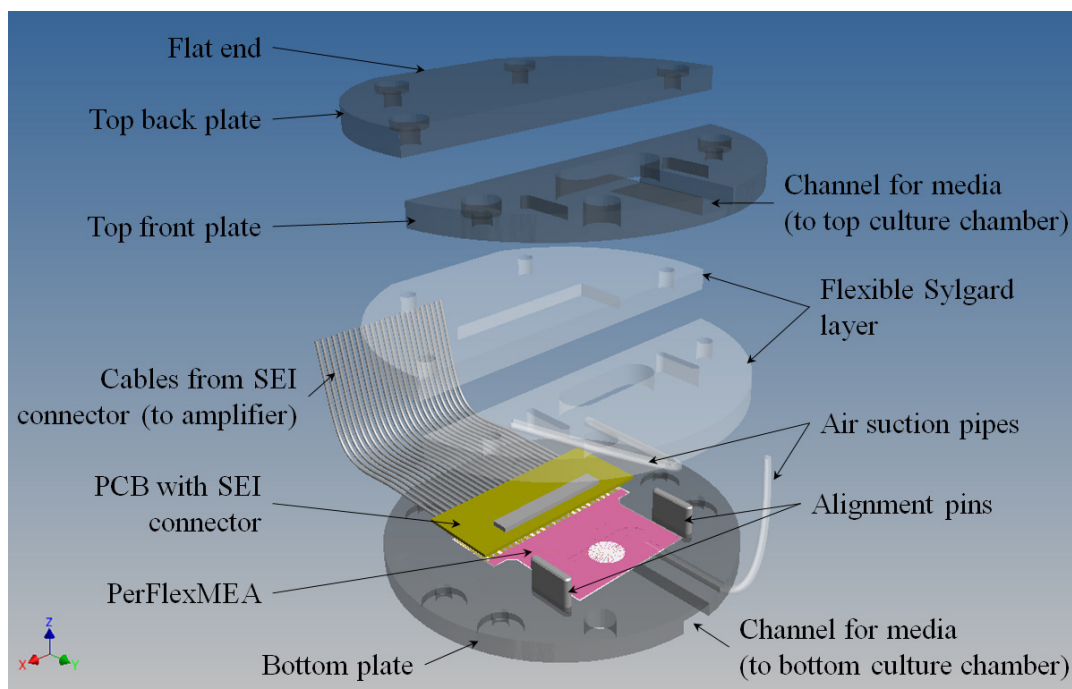


Figure 5.3 Exploded view of the coin setup for housing the PerFlexMEA. The PerFlexMEA was located on the bottom plate with the cell culture zone falling in the culture chambers of the top and bottom plate. The SEI contacts molded in Sylgard, interfaced with the contact pads of the PerFlexMEA. The flexible Sylgard layer was sandwiched between the rigid PCTE plates (top and bottom plates). Channels were provided to each cell culture chambers to allow the flow of media into them. Air suction pipes were provided to remove air bubbles from whichever chamber faces bottom. View was produced using Autodesk Inventor Professional 2011.

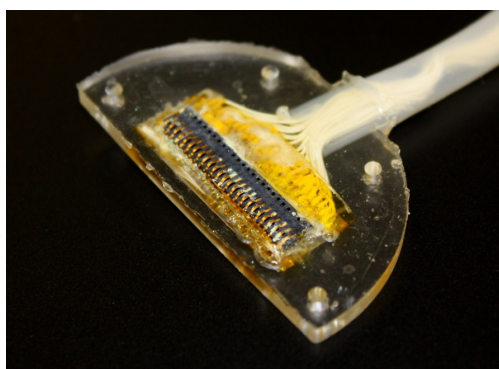


Figure 5.4 SEI one piece interface molded in Sylgard® with cables leaving from the flat end. The SEI interface and wires were soldered into a thin circuit board. The wires were enclosed in a pipe that isolates them from the media at the flat end.

## 5.2 Amplifier and Recording System

The amplifying and recording system consisted of four components:

- (1) *Signal amplification and recording system*. – Amplified the recorded signal to study the signal deflections in more detail.
- (2) *Temperature control system* – Maintained the temperature of the preparation using a micro-incubator and temperature controller.
- (3) *Noise reduction set up* – Insulated and minimized signal noise from the environment and other external sources.
- (4) *Computer-user interface* – Collected and visualized the signals generated by the cellular preparation.

Figure 5.5 shows the components and design of the complete setup for a recording experiment.

### 5.2.1 Signal Amplification and Recording System

A existing MEA60 amplifier system<sup>3</sup> was employed for our recording. The MEA60 amplifier system was capable of recording from 60 electrodes simultaneously and had an automated gain control system. The system set the gain values based on signal magnitude and noise. A convertible connector was designed to utilize 20 recording channels of the MEA 60 system (Figure 5.6). The corresponding recording pins were organized into a  $5 \times 4$  signal array for computer display. The amplifier was connected to the data acquisition computer via a single 68-pin MCS standard cable. A separate chloridized silver wire immersed in the media and connected to the amplifier system worked as a general ground.

---

<sup>3</sup> Multi Channel Systems, Reutlingen, Germany

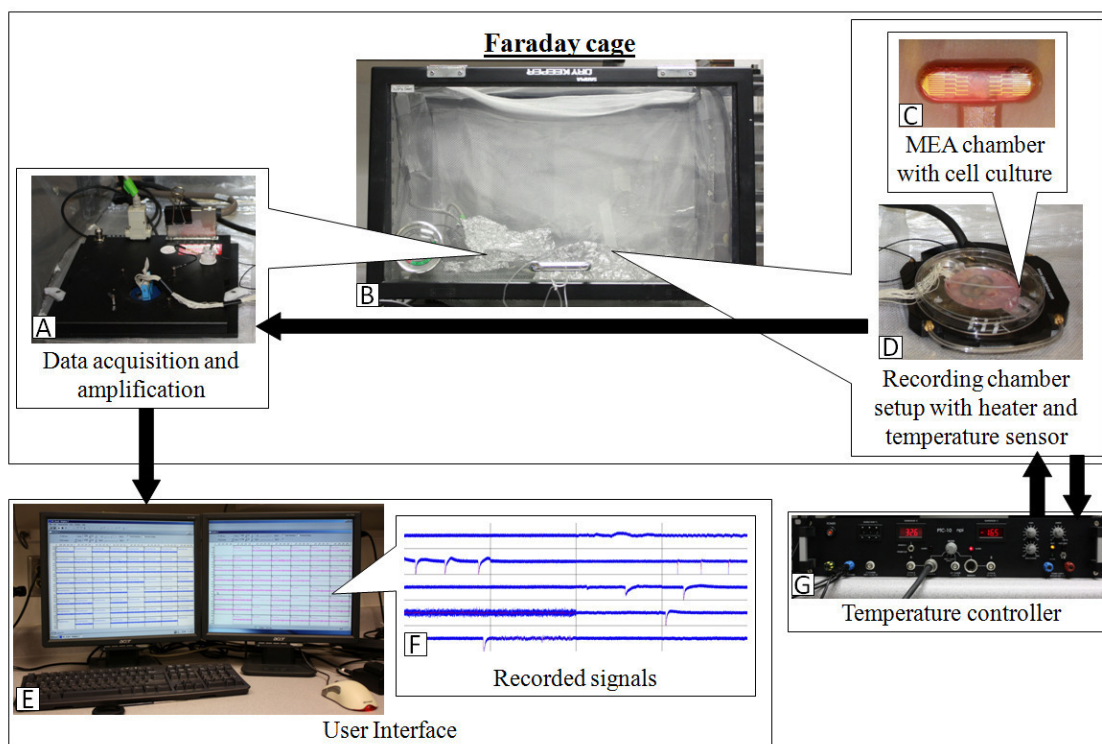


Figure 5.5 The Amplifier and recording setup (A) MEA60 amplifier system with the 20-pin converter. (B) Faraday cage housing the amplifier and micro-incubator setup. The amplifier and micro-incubator setup was covered with grounded aluminum foil to enhance shielding. (C) Cell culture chamber in the coin. (D) The coin placed in a 60mm Petri dish placed in a micro-incubator and covered with a 100mm Petri dish lid. (E) Recorded signals as displayed by the MCRack software installed in the computer. (F) Recorded signals from the preparation (G) Temperature controller for the micro-incubator.

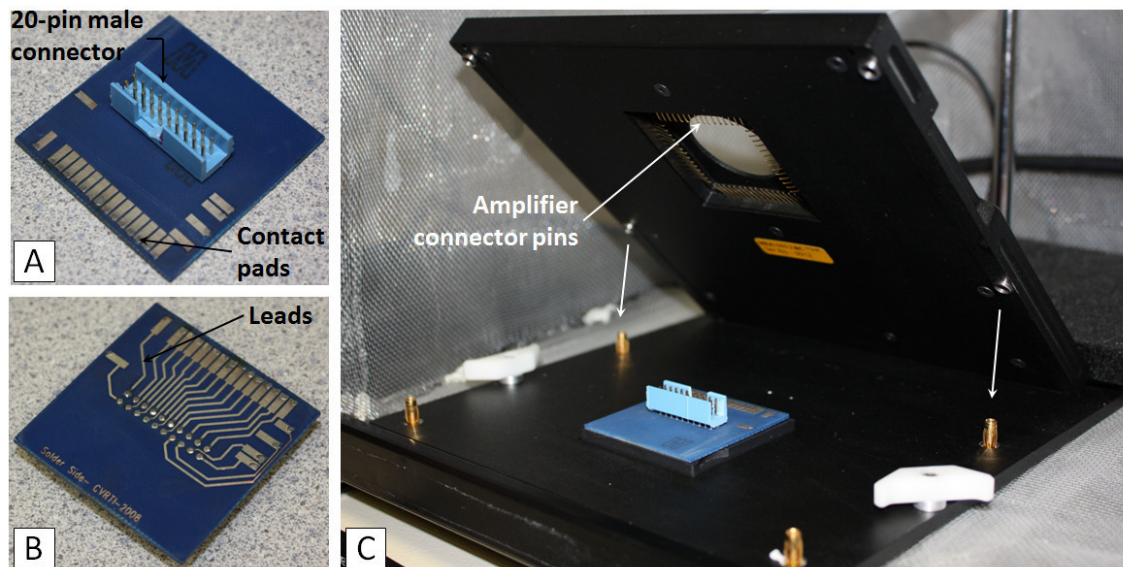


Figure 5.6 The 20-pin convertor for the MEA60 system. (A) View of the top side of the 20-pin convertor. The female connector from the coin setup goes into the 20-pin male connector at the centre. The amplifier connector pins sit on the contact pads at the edge of the connector. (B) View of the bottom side of the 20-pin connector. The 20-pin connector was connected to the contact pads by leads in the bottom side. (C) The 20-pin convertor located in the MEA60 amplifier system in place of the MEA. The amplifier has 4 alignment pins to align the amplifier connectors to the 20-pin convertor.

### 5.2.2 Temperature Control System

The 60mm Petri dish holding the coin setup was positioned in a customized HCMIS micro-incubator<sup>4</sup>. The micro-incubator maintained the preparation at temperatures between 37-38°C using a PTC-10 (Peltier Temperature Control) system<sup>5</sup>.

### 5.2.3 Noise Reduction Setup

The Petri dish containing the PerFlexMEA setup was shielded with grounded aluminum foil to minimize electromagnetic noise in the recorded signal. The complete recording setup – PerFlexMEA, micro-incubator and MEA amplifiers – were placed in an

<sup>4</sup> ALA Scientific Instruments, Inc., Farmingdale, USA

<sup>5</sup> npi electronics GmbH, Tamm, Germany

enclosed box with inner walls covered with aluminum mesh that functioned as a Faraday cage. This further increased shielding against stray noise from the outside environment.

#### 5.2.4 Computer-user Interface

MCRack software<sup>4</sup> was customized to observe and save the recorded signals from the 20 electrodes.

## CHAPTER 6

### PERFORMANCE EXPERIMENTS

A set of experiments was designed to validate each of the functional objectives (discussed in Section 3.1) of the PerFlexMEA. The following experiments were conducted to validate the functionality of the fabricated device.

#### 6.1 Biocompatibility

For any instrument to work in a biological environment, it should be able sustain the biological specimen. In our specific case, it is important to determine that the selected materials do not interfere with the physiology of the cells under study. As an initial test, a cell growth experiment was conducted.

##### 6.1.1 Cell Growth Experiment

The main objective of this experiment was to compare the growth rate of a selected cell line in control conditions or under the influence of our fabrication materials as a fine index of possible effects of our materials on cellular physiology. Figure 6.1 presents the simplified representation of the experiment. To start with,  $50,000 \pm 2500$  HeLa WT cells were plated in three sets of five 35mm Petri dishes each. The first set was



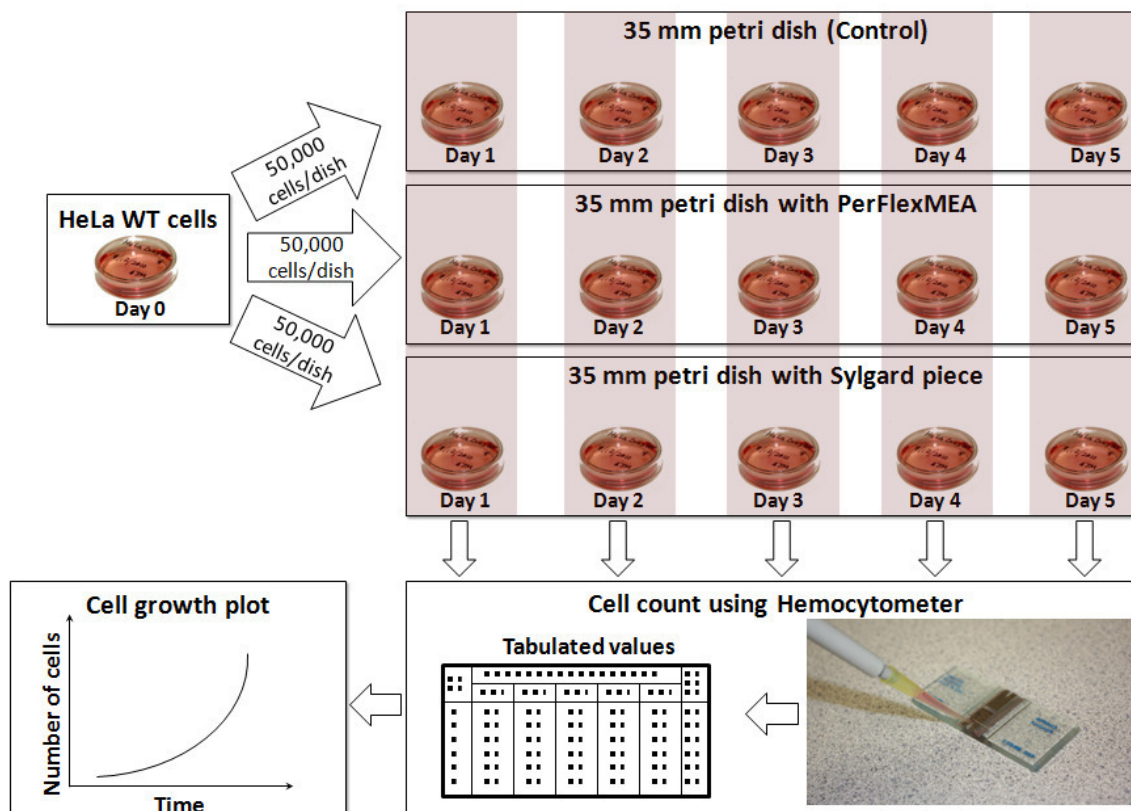


Figure 6.1 Basic steps of cell growth experiment. HeLa WT cells were plated in 3 sets of 5 Petri dishes. One set was control while the other two had pieces of PerFlexMEA and Sylgard respectively. Cells were counted from each set during the following 5 days using a hemocytometer. The cell counting data was tabulated and plotted to determine cell growth rates.

used as control. Small 33 mm pieces of PerFlexMEA and Sylgard were placed in the second and third set, respectively. Cell number was calculated every day from each set using a hemocytometer during the following 5 consecutive days. The data were plotted and compared.

### 6.1.2 Experiment Results and Discussion

Figure 6.2 shows a time vs. cell concentration plot for the three sets. All three curves increase exponential-like until day 4-5, when the cell concentration rate reduces or

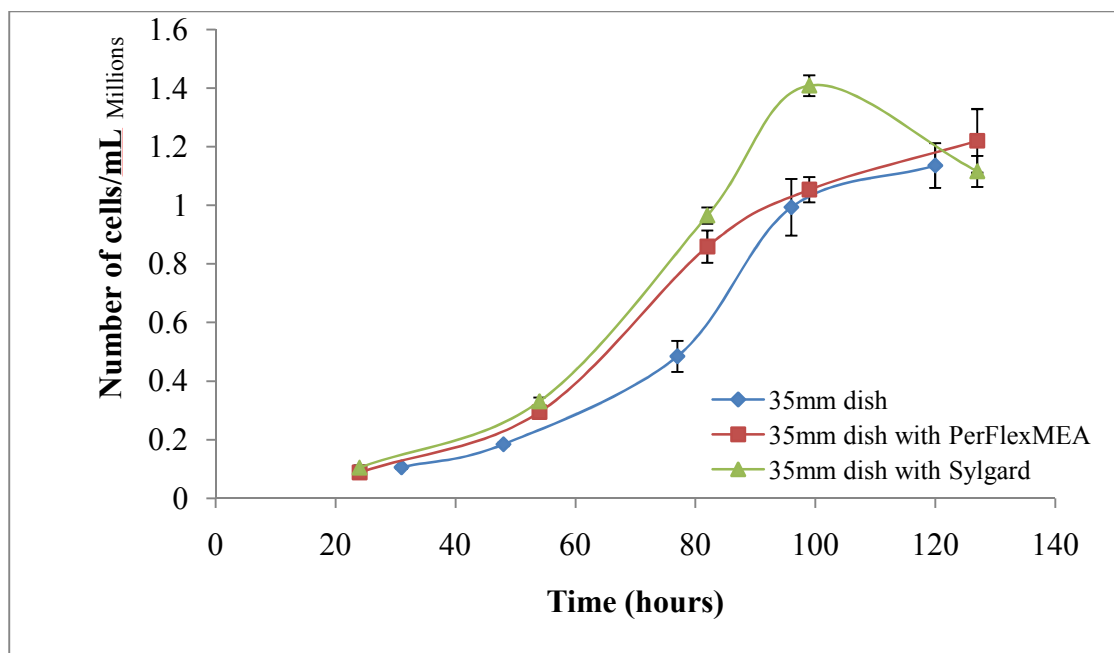


Figure 6.2 Cell growth experiment result. The cell count from each preparation for 5 days is plotted. The standard error bars represent the variation from 3 distinct counts from the particular day's preparation. Cell growth for all conditions appears to be exponential-like. The curves tend to reach a maximum after 4 days and are similar to control, indicating that by themselves, Sylgard and the PerFlexMEA are biocompatible.

even drops in one case (with Sylgard). The reduction in growth rate (and drop in one case) is probably due to cell overcrowding in the 35mm Petri dish. As a result of overcrowding, cells detach and float on the media and get discharged when washing the cells. The observed differences in the curves can be accounted by the variation in initial number of cells plated. Since the cell growth follows geometric proportion, a small variation in the initial number creates a large difference after long duration.

In general, the cells grew as expected. The growth rate for Sylgard and PerFlexMEA are comparable and larger compared to control. No abnormal reduction in cell growth was observed. Therefore, the selected materials are biocompatible and capable of sustaining cell cultures.

## 6.2 Cell Coupling Across the Membrane

The second functional objective concerns cell to cell communication across the membrane. Cell to cell communication involves the physical connection of cells to each other which permits the movement and transfer of intracellular material or signaling to each other. A cell drop experiment was conducted using fluorescent dyes to confirm cell to cell communication across the membrane.

### 6.2.1 Cell Drop Experiment

HeLa Cx43 cell type was selected for the cell drop experiment. HeLa Cx43 is known to communicate with neighboring cells of the same type through gap junction channels. On day 0, cells were stained with DiI<sup>1</sup> and plated on the electrode side of the PerFlexMEA. DiI is a hydrophobic fluorescent molecule that partitions in the cell membrane and fluoresces red (fluorescence emission maximum at 565nm) when exposed to UV light. The cells can be spotted under the microscope using a red filter. DiI dye is soluble in the cellular membrane, and although it can diffuse around the cell, it has not been observed to diffuse into membranes from contiguous cells (e.g. cellular secretion, pinocytosis or phagocytosis can allow the dye to go into other cells but it takes several days). On day 1, the membrane was turned over and plated with another set of HeLa cells. These cells were loaded with CellTracker<sup>TM</sup> Green CMFDA<sup>2</sup> (also known as Green Tracker). Green Tracker is able to pass freely through the cell membrane. Green Tracker by itself does not fluoresce, but once inside, it reacts with intracellular esterases to form a fluorescent membrane impermeant molecule. When exposed to UV light, the newly

---

<sup>1</sup> Molecular Probes cat #D282

<sup>2</sup> Molecular Probes cat #C7025

formed molecule fluoresces green (maximum at 517 nm) and can be spotted under the microscope using a green filter. This fluorescent molecule can move along within the cytoplasm. The molecular dye is small (379 Dalton) and can diffuse across gap junction channels. If intercellular communication is established between cells, the dye molecule can diffuse and be spotted in surrounding cells after 6 to 8 hours in co-culture.

For this experiment, a three-layered preparation was used, where the membrane was sandwiched between red and green-stained HeLa Cx43 cells. The cell-membrane preparation was incubated for 6-8 hours. After incubation, the preparation was observed under the microscope in UV light through red and green filters. Since the green dye molecules can move, red stained cells with green dye would indicate coupling across the two cellular layers through the recording membrane.

### 6.2.2 Experiment Results and Discussion

HeLa Cx43 cells were successfully plated on both sides of the recording membrane and showed normal cell growth on visual inspection under the microscope. Since the width of the whole preparation was about 30 $\mu$ m, both cell layers could not be focused simultaneously. Therefore, each cell layer was viewed after modifying the microscope focus. This characteristic was helpful in identifying the cells in the bottom layer (red stained) that received the green dye. Using the red filter, the microscope was focused to the red stained cells' level. The filter was changed to green and cells that appeared focused with the green dye were spotted. The microscope was then focused to the top layer to identify the prospective donor cell across the membrane. Multiple pairs of cells that transferred the green dye across the membrane were spotted. Figure 6.3 shows

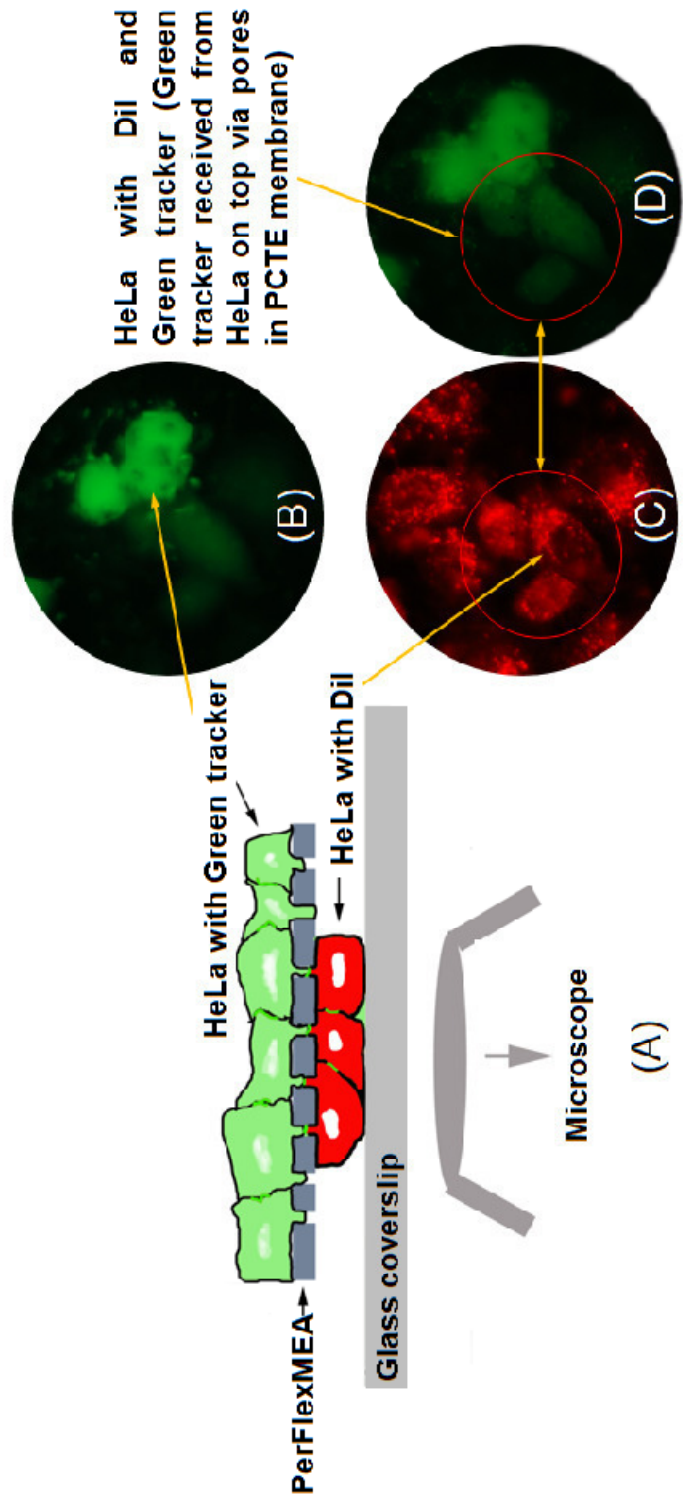


Figure 6.3. Cell drop experiment. (A) The PerFlexMEA was sandwiched between green stained and red stained HeLa Cx43 cells. B, C and D show the microscope views using green (B and D) and red filters (C). In B the microscope was focused onto the top layer (green stained cells visible with green filter). Few blurred green cells were also visible. In C the microscope was focused to the bottom layer of cells (red stained cells visible with red filter). The green cells are not visible. In D the microscope is focused to view the bottom layer of cells but viewed via the green filter. The same red cells (circled with red in C and D) appear as sharp green cells. The cells circled with red (in C and D) represent the red stained cells with green dye.

one such case. This confirms cell to cell communication across the membrane which occurs only through gap junction. Therefore, the PerFlexMEA permits the formation of gap junctions across the membrane between the co-cultured cells.

### 6.3 Electrophysiological Recording

A recording experiment was setup utilizing the existing MEA60 system to determine if the device was capable of recording electrical signals from cardiomyocytes.

#### 6.3.1 Recording Experiments using MEA60 System

The recording experiments were conducted at the Connexin Lab, Nora Eccles Cardiovascular Research and Training Institute (CVRTI), University of Utah. The PerFlexMEA was assembled into the coin setup to protect the membrane and isolate the recording electrodes from the contact pads (the coin setup; Figure 5.2). The complete and assembled coin setup was washed with PBS and ethanol, and dry-autoclaved at 120 °C. The coin setup was then placed in a 60mm Petri dish to maintain the cells in culture. Before plating the cells, the membrane was hydrated and treated with fibronectin. Hydration of membrane was achieved by leaving the coin setup in PBS solution for 6-8 hours. Fluid soaks through the air filled pores of the membrane, allowing fluid movement across the membrane. Air, if not removed, hinders cell functioning and prevents the formation of gap junction across the membrane. Fibronectin promotes cell adhesion to the membrane surface. The PerFlexMEA membrane was soaked for 1 hour before plating cells in 2 µg/ml fibronectin solution for 45-60 minutes to promote cell adhesion to the membrane. Neonatal myocytes were isolated and the equivalent to 6-8 hearts were plated

on one side of the culture chamber. 300  $\mu$ M BRDU was added to the culturing media (DMEM) to restrict fibroblast growth. (DMEM solution : HyQ DMEM/High Glucose<sup>3</sup>; 10% FBS Fetal Bovine Serum<sup>4</sup>, 1% Pen Strep [10000 ui Penicilin, 10,000 ug/ml Streptomycin, 25 ug/ml Amphoterecin B]<sup>5</sup>, 1% L-Glutamine 200mM<sup>6</sup> and 1% Non-essential-amino acids<sup>7</sup>).

Once the cells were plated, the coin setup was left in the incubator (37°C, 6% CO<sub>2</sub>, moisture) for 36-48 hours. This gave cells ample time to adapt to the new conditions. Culture media was changed every 48 hours.

Before electrophysiological recordings, the culture media was exchanged for OptiMEM (DMEM with Hepes pH buffer<sup>8</sup>) and incubated for 60-90 minutes for acclimatization. OptiMEM allows long recordings outside a 6% CO<sub>2</sub> atmosphere. After acclimatization, the 60mm Petri dish holding the coin setup was positioned in a customized HCMIS micro-incubator<sup>9</sup>. The micro-incubator maintained the preparation at temperatures between 37-38°C. The connector from the PerFlexMEA was plugged into the MEA amplifier using the designed 20 electrode connector. The signals from the preparation were recorded and stored using the MCRack software on the computer. Recordings were taken at a sampling rate of 5 kHz. After recordings were completed, the PerFlexMEA was unplugged from the recording system; the culture media in the Petri dish was changed back to 300  $\mu$ M BrdU DMEM solution and left for incubation.

---

<sup>3</sup> Hyclone # SH30243.01

<sup>4</sup> Hyclone # SH 30070.03

<sup>5</sup> Cellgro # 30-004-C1

<sup>6</sup> Cellgro # 25-005-C1

<sup>7</sup> Sigma #M7145

<sup>8</sup> Gibco # 31985

<sup>9</sup> ALA Scientific Instruments, Inc., Farmingdale, US

### 6.3.2 Experiment Results and Discussions

Figure 6.4(A) shows the signals recorded from the 20 recording electrodes on the PerFlexMEA on day 1 after plating. The signal in blue represents the raw signal, while those in pink are low pass filtered. Signals recorded at electrodes 21, 24, 33, 34, 44 and 51 can be clearly identified as action potentials (refer to Figure 2.2) [1]. Action potential shape was also comparable to signals recorded from cardiomyocyte preparation in a standard MEA. Figure 6.4(C)-(D) show one such selected pair of action potentials from the PerFlexMEA and standard MEA. The recorded signal from the PerFlexMEA was much noisier than from the standard MEA. Figure 6.4(B) shows a constant beat rate of 33 beats per minute. The identified action potentials measured a signal to noise ratio (*SNR*) of 8.6 and peak to peak voltage ( $V_{pp}$ ) of 200  $\mu$ V.

### 6.4 Summary

Each of the experiments furnished positive results. The PerFlexMEA and Sylgard showed normal cell growth rate, hence biocompatible. The cell drop experiment exhibited cases where fluorescent dye movement from cell to cell across membrane was observed. This confirmed gap junction formation between cells cultured across the membrane. The cell drop experiment also exhibited co-culturing cells, though of the same type, on both sides of the PerFlexMEA. Finally, spontaneous electrical activity signals were recorded from a cardiocyte culture and action potentials identified, demonstrating the device's capability of recording from excitable cultured cells.



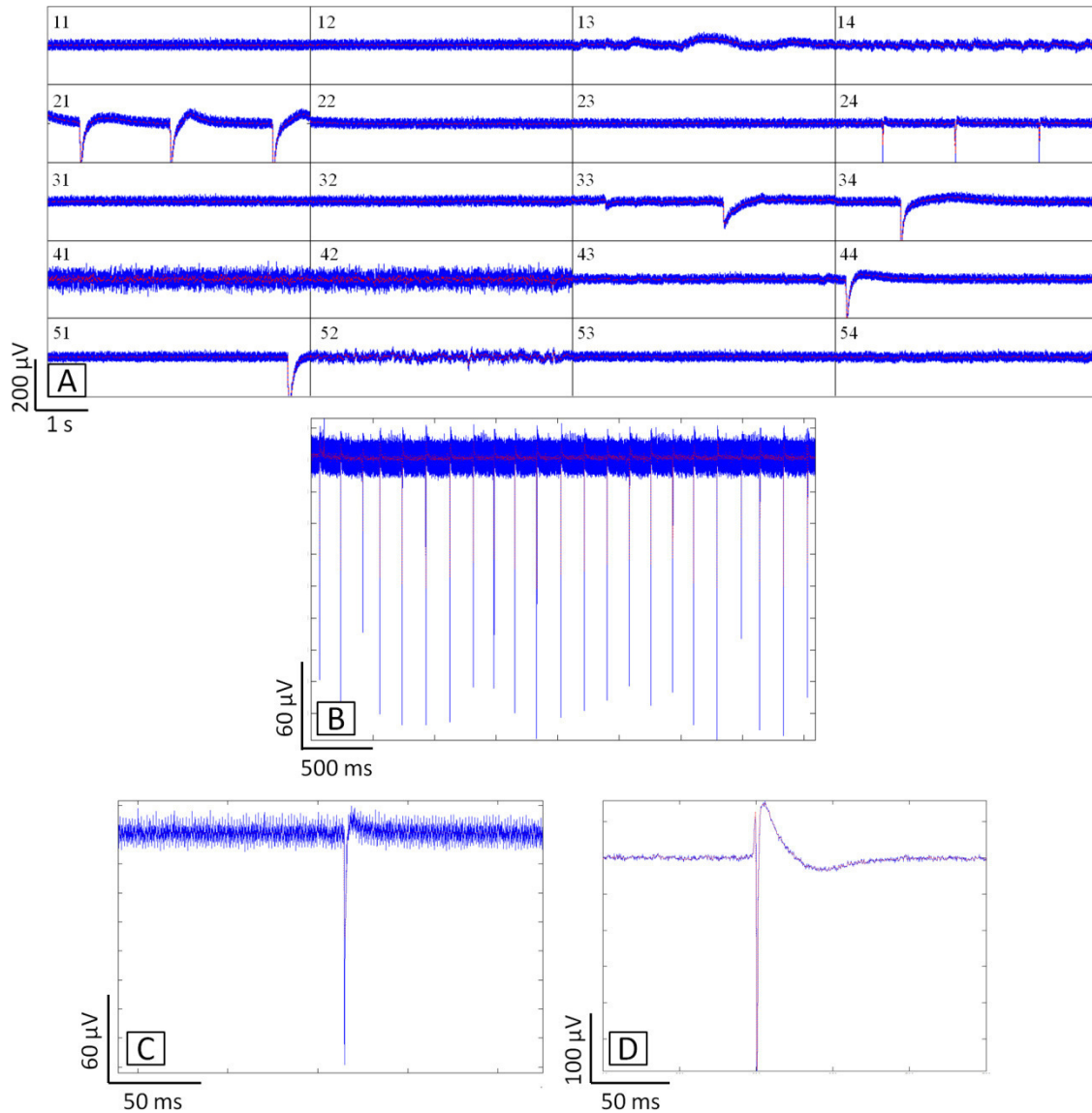


Figure 6.4. Recorded signals from a PerFlexMEA. Cardiocytes were plated on the electrode side. (A) Recording from the 20 electrodes of the  $4 \times 5$  array ( $\Delta t = 5$  s). Note that electrodes 21 and 24 are recording at the same rate, indicating that the cells on top of these electrodes might be electrically coupled. (B) Chronic single electrode recording showing constant beat rate ( $\Delta t = 42$  s). (C) Action potential close up recorded from a PerFlexMEA electrode ( $\Delta t = 250$  ms). (D) Action potential close up recorded from a standard MEA ( $\Delta t = 250$  ms).

### 6.5 References

- [1] M. Halbach, *et al.*, "Estimation of action potential changes from field potential recordings in multicellular mouse cardiac myocyte cultures.," *Cell Physiol Biochem*, vol. 13, pp. 271-84, 2003.

## CHAPTER 7

### RESULTS SUMMARY, CONCLUSIONS, FUTURE WORK AND APPLICATIONS

#### 7.1 Results Summary

The PerFlexMEA was designed and fabricated within the specified design constraints and successfully recorded electrical signals from isolated neonatal cardiocytes. A fabrication technique was effectively devised for patterning recording electrodes on the flexible porous polycarbonate substrate without losing membrane porosity at selected regions. A coin setup was designed and manufactured to house the PerFlexMEA. The complete setup – PerFlexMEA and coin setup, showed normal cell growth rate with HeLa WT cells, demonstrating biocompatibility of the complete setup. Cells were successfully co-cultured on both sides of the PerFlexMEA and formed gap junctions across the membrane. The existing MEA60 amplifier system was successfully interfaced to the PerFlexMEA for performing recording experiments. Cardiomyocytes, isolated from neonatal mice, were plated on the recording side of PerFlexMEA and electrical activity was recorded.

## 7.2 Conclusions

The PerFlexMEA presented here constitutes a new MEA device. It is capable of recording electrical signals from a preparation where two cell types can be easily co-cultured in two independent chambers while permitting cell to cell communication between the cell types. Though dye communication across the PerFlexMEA amongst only one cell type was presented, the capability of the device to separately co-culture cells on both sides has been established. The PerFlexMEA presents itself as a new tool for studying excitable cell activity. It simplifies the method for co-culturing cells in two independent chambers on a recording device for studying the effects of varying cell distribution in excitable tissues.

A new method for patterning metals and insulators on a porous flexible substrate while maintaining its porosity has been also presented. This method has been effectively utilized and streamlined for PerFlexMEA fabrication.

The materials used for the PerFlexMEA fabrication were biocompatible with HeLa cells and cardiocytes supporting the possibility of using this device not only for *in vitro* research but also in damaged tissue regeneration and transplantation.

## 7.3 Future Work

### 7.3.1 Design

The coin assembly for packaging and interfacing has 22 parts (including 6 pairs of nylon screws and nuts). This makes it extremely vulnerable to contamination during assembly. Furthermore, the complete coin setup needs to be placed entirely in the media. This makes it prone to contamination during handling. A simpler approach involving

fewer parts can be designed by reducing the number of parts kept wet in the media. One possible solution would be to fabricate a longer PerFlexMEA where the cell culture and contact zones are placed farther apart and only the electrodes are immersed in the media while the contacts are maintained dry outside the Petri dish. This would significantly reduce vulnerability to contamination.

### 7.3.2 Cell-Specific Recipes

Different cells respond differently to a selected substrate material. For example, the HeLa and N2A cells easily adhered to the PerFlexMEA, forming a monolayer of cells. This was not the case with cardiomyocytes where cell adhesion was partial and the membrane had to be overloaded with cells to improve results. This is not the case either when plating cells on glass (commercial MEAs) or polystyrene (lab Petri dishes) substrates. Therefore, a specific recipe for treating the membrane surface to promote cardiomyocyte adhesion to our new device needs to be developed by testing molecular substrates like collagen, laminin and fibronectin at different concentrations. Likewise, other cell-specific recipes will be necessary to be developed for other other cell types.

## 7.4 Future Applications

The PerFlexMEA is capable of co-culturing two types of cells simultaneously in a controlled and simple manner and recording from one side. It is potentially a useful tool in the study of excitable tissues like those in the heart, brain, muscles, etc. While in this thesis it has been used for *in vitro* experiments, the electrode array device can be also designed for recording *in vivo*. The highly flexible and porous substrate could be

effective in reducing tissue damage and trauma like most flexible electrode array devices (discussed in Section 2.2.4).

Current cell patterning techniques only enable the control of cell number and distribution cultured in 2D. 3D Scaffolds enable creating cultures in 3D but without much control of cellular and spatial distribution. The PerFlexMEA presents a means by which cells can be potentially cultured in 2D layers which are subsequently stacked to form 3D structures. Such advancements could help in constructing *in vivo* like *in vitro* tissue preparation, which would evade the challenges faced during *in vivo* applications. Such 3D MEA systems would also serve as a key tool in tissue engineering. Most tissues are made of two or more cells types, for example brain: glia and neurons, heart: fibroblasts and myocytes, veins: endothelia and smooth muscle cells. Artificially generating such tissues would require electrode systems which facilitate the study of the effects of communication between different cell types on the propagation of action potentials in two and three dimensions. Such multielectrode systems would need perforated membranes to allow intercellular communication and proper circulation of nutrient perfusions and tissue fluids. Microfluidics will play a vital role in the development of systems for delivering and maintaining nutrient perfusions.

The use of a biodegradable membrane for the PerFlexMEA substrate could allow us to use it in transplants where the recording system may stay in place. The biodegradable membrane would act as a scaffold until the cells form a self-sustaining tissue. This would be very useful for monitoring cellular activity during and after organ regeneration.

### 7.5 Contributions and Outcomes

- Alonso P. Moreno, Gary S. Goldberg, Abhijit Mondal, Ian R. Harvey and Brian Baker, “**Cultured Tissue Rolls for 3 Dimensional Electrical Recording and Tissue repair**”, *filed for United States Patent (July 2010)*.
- Abhijit Mondal, Alonso P. Moreno, Ian R. Harvey, Brian Baker, **PerFlexMEA: A multielectrode array for cell culture on a thin perforated flexible polycarbonate membrane**, 6<sup>th</sup> Annual Mountain West Biomedical Engineering Conference 2010.
- Abhijit Mondal, Alonso P. Moreno, Ian R. Harvey, Brian Baker. **PerFlexMEA: A multielectrode array for cell culture on a thin perforated flexible polycarbonate membrane**, *in preparation, 2011*.

## APPENDIX A

### MICROFABRICATION PROCESS PARAMETERS

Tables A.1 to A.6 present the process parameters set on the various systems used for the fabrication of PerFlexMEA.



Table A.1 PDS 2010 parylene coater process parameters for parylene – layer 1 deposition.

Parylene dimer weight	0.9 g
Furnace temperature	690 °C
Chamber gauge	135 °C
Vaporizer	175 °C
Vacuum	25 mTorr

Table A.2 Plasmalab 80 Plus process parameters for parylene (layer 1) surface etch.

Base pressure	$4 \times 10^{-4}$
CM gauge pressure	0.105 Torr
Substrate temperature	6 °C
Oxygen gas flow rate	50 sccm
Etch time	30 s

Table A.3 TMV Sputter system process parameters

	Layer 1	Layer 2	Layer 3
Order of deposition	Titanium (Ti)	Titanium dioxide (TiO <sub>2</sub> )	Gold (Au)
Main chamber base pressure	$3.2 \times 10^{-7}$ T	$3.2 \times 10^{-7}$ T	$3.2 \times 10^{-7}$ T
Target materials	Ti	Ti	Au
Process gases	Ar	Ar/O <sub>2</sub>	Ar
Gas flow rate	150 sccm	150/100 sccm	150 sccm
Deposition pressure	8 mT	8 mT	5 mT
Power source type	RPG	RPG	DCG
Pre-sputter power	45 w	45 w	50 w
Deposition power	45 w	45 w	50 w
Deposition times	90 s	90 s	300 s

Table A.4 Electromask PG/IR system.

Mask size	5" × 5"
Type	5206
Exposure value	950

Table A.5 PDS 2010 parylene coater process parameters for parylene layer – 2 deposition.

Parylene dimer weight	0.9 g
Furnace temperature	690 °C
Chamber gauge	135 °C
Vaporizer	175 °C
Vacuum	25 mTorr

Table A.6 Plasmalab 80 Plus process parameters for parylene patterning (layer 1 + layer 2).

Base pressure	$4 \times 10^{-4}$	
CM gauge pressure	0.105 Torr	
Substrate temperature	6 °C	
Oxygen gas flow rate	50 sccm	
Process power	RF forward power	200 w
	RF reflected power	2.8 w
Etch time	420 s	

## APPENDIX B

### CHARACTERIZATION

Table B.1 presents the layer thicknesses of the different layers deposited as measured on an auxiliary sample using Tencor P-10 profilometer.

Table B.1 Thickness of different layer deposition measured from auxiliary samples using Tencor P-10 profilometer.

	Samples	Thickness (nm)					Mean (nm)	Standard Deviation (nm)	Standard Error (nm)
		1	2	3	4	5			
Parylene (layer 1)	1-3	450	470	490	440	430	460	20	10
	4-6	500	520	480	500	490	500	20	10
Au + TiO <sub>2</sub> + Ti	1-6	170	130	100	140	110	130	30	10
Parylene (layer 2)	1-3	480	540	500	540	500	510	30	10
	4-6	600	620	560	600	560	590	30	10

## APPENDIX C

### CELL GROWTH EXPERIMENT DATA

Tables C1 to C3 tabulate the data from the cell counting experiments for studying cell growth rate using HeLa WT cells.

## C.1 Cell count from control Petri dish

35 mm Petri dish (controls)								
Day	Time of day	Time (hrs)	Cell Concentration in 0.5 mL cell suspension solution ( $\times 10^3$ cells/mL)			Mean ( $\times 10^3$ cells/mL)	Standard Deviation ( $\times 10^3$ cells/mL)	Standard Error ( $\times 10^3$ cells/mL)
			1	2	3			
1	7:00 PM	31	114	98	105	105	8	5
2	12:00 PM	48	179	178	196	184	10	6
3	5:00 PM	77	588	414	452	485	91	53
4	12:00 PM	96	1051	1124	805	993	167	96
5	12:00 PM	120	1190	1232	985	1135	132	76

## C.2 Cell count from Petri dish with PerFlexMEA

35 mm Petri dish with PerFlexMEA								
Day	Time of day	Time (hrs)	Cell Concentration in 0.5 mL cell suspension solution ( $\times 10^3$ cells/mL)			Mean ( $\times 10^3$ cells/mL)	Standard Deviation ( $\times 10^3$ cells/mL)	Standard Error ( $\times 10^3$ cells/mL)
			1	2	3			
1	12:00 PM	24	95	95	75	88	12	7
2	6:00 PM	54	336	282	264	294	38	22
3	10:00 PM	82	890	935	752	859	95	55
4	3:00 PM	99	1038	1135	988	1053	75	43
5	7:00 PM	127	1398	1240	1022	1220	188	109



## C.3 Cell count from Petri dish with Sylgard®

35 mm Petri dish with Sylgard®								
Day	Time of day	Time (hrs)	Cell Concentration in 0.5 mL cell suspension solution ( $\times 10^3$ cells/mL)			Mean ( $\times 10^3$ cells/mL)	Standard Deviation ( $\times 10^3$ cells/mL)	Standard Error ( $\times 10^3$ cells/mL)
			1	2	3			
1	12:00 PM	24	118	89	108	105	15	8
2	6:00 PM	54	352	333	307	331	22	13
3	10:00 PM	82	1000	985	910	965	48	28
4	3:00 PM	99	1338	1440	1447	1408	61	35
5	7:00 PM	127	1220	1078	1050	1116	91	53

## APPENDIX D

### ISOLATION OF NEONATAL CARDIOMYOCYTES

### Cell Isolation for *In Vitro* Experiment

Neonatal mouse CD-1 pups (0-2 days old) were anesthetized (furane vapors) and their skin sterilized with 70% ethanol. Pups were immediately decapitated and their hearts excised. Atria and nonventricular tissue was removed. Ventricles were minced with scissors (for about 5 times) and placed in oxygenated DMEM to prevent ischemia. All collected ventricles were scissors-minced further submerged in digesting enzyme solution (filter sterilized solution containing 4:1 3% BSA (bovine serum albumina; Amesco # 9048-46-8) in PBS:Ham's F10 (Invitrogen # 11550-043) with approx. 1320 units/ml Collagenease type I [Wothington LS004196]) in an 1.5 ml Eppendorf tube for 2 minutes until they broke into considerably small pieces. The finely minced hearts were transferred into a 35mm dish with the digestive enzyme solution and incubated for 15 minutes at 37 °C under constant shaking (150 rpm) until the tissue-enzyme solution turned fuzzy/cloudy. All Petri dish's contents were centrifuged at 180g at room temperature for 2 minutes and the supernatant removed. The residual pellet was washed in 1% BSA in F10 (1% F10) solution and centrifuged again as in the previous step. After supernatant removal, the residual pellet was resuspended in 1% F10 solution using a transfer pipette. The suspension was filtered though a 70 $\mu$  filter, centrifuged at low speed for 2 minutes at room temperature and resuspended in 500  $\mu$ l F10 media. A Ficoll gradient (5 layers of 1.09, 1.06, 1.03, 1.00, 0.97 densities in F-10) was prepared in a Beckman high speed 1.5 ml tube using 150  $\mu$ l of each layer dispensed gently in decreasing order of density. Cells were layered on top of the gradient. The gradient contents were spun at 47000g (approximately 19000 rpm) and 22 °C for 8-10 minutes in a JA-20 rotor (J2-HS centrifuge, Beckman Coulter, Inc., Brea, US). This separated the

viable cardiocytes from red blood cells and debris by forming discrete layers in the Ficoll gradient. The top layer is removed exposing the myocyte layer, which was then collected in a 200  $\mu$ l pipetman. The recovered cells were washed in 1% F10 solution and spun at low speed and room temperature for 2 minutes. The supernatant was removed and the pellet resuspended in 1% F10 solution using a transfer pipette. The suspension was then filtered through a 40 $\mu$  cell strainer and pelleted by low speed centrifugation. After supernatant removal, the pelleted cells were resuspended in DMEM-CM and transferred into a 60 mm Petri dish that was then incubated (37 °C, 6% CO<sub>2</sub>) for approximately 45 minutes until fibroblast adhesion was observed (using 20x microscope). Once fibroblast adhesion was observed, the myocyte-rich media was removed and pelleted by low speed centrifugation. The myocytes were resuspended in 300  $\mu$ M BrdU DMEM solution (BrdU controls fibroblast growth) and plated on an appropriate recording substrate (MEA or PerFlexMEA).